



Asymmetric conjugate addition reactions with chiral oxadiazinones: Unusual conformational properties of the oxadiazinones



Fatima Olayemi Obe, Ryan A. Davis, Jennifer Spurlock, Morgan M. Grunloh Barnes, Tyler Lindvall, Micah S. Wendorf, Christina Delach, Gregory M. Ferrence, Jean M. Standard^{**}, Shawn R. Hitchcock^{*}

Department of Chemistry, Illinois State University, Normal, IL, 61790-4160, USA

ARTICLE INFO

Article history:

Received 26 November 2020

Received in revised form

25 January 2021

Accepted 2 February 2021

Available online 12 February 2021

Keywords:

Oxadiazinone

Chiral auxiliary

Asymmetric conjugate addition

Conformational analysis

Computational

ABSTRACT

A series of *Ephedra* based oxadiazinones have been prepared, acylated, and examined in the asymmetric conjugate addition reaction with Grignard reagents in the presence of copper(I) bromide-dimethyl sulfide complex. The highest diastereoselectivity that was obtained in the conjugate addition reaction was observed with the (1*R*,2*S*)-ephedrine based *N*₄-methyloxadiazinone (5:1 d.r.) favoring the formation of the (*S*)-configuration of the conjugate addition product. Efforts to enhance the level of diastereoselection via increasing the steric volume of the stereo-directing *N*₄-substituent of the oxadiazinone (*N*₄ = *p*-methoxyphenyl or -isopropyl) led to an observed decrease in the level of diastereoselection. A computational study was conducted to examine the conformations adopted by the *N*₄-methyloxadiazinone vs. the *N*₄-isopropyl-oxadiazinone that yielded the lower diastereoselectivity. An argument is made for the stereoelectronic properties of the *N*₄-substituent being the cause of both the moderate diastereoselectivity and the unexpected facial preference for the conjugate addition.

© 2021 Elsevier Ltd. All rights reserved.

1. Introduction

The stereoselective formation of new carbon-carbon bonds by the process of asymmetric conjugate addition represents an important class of reactions in synthetic organic chemistry [1]. While catalytic methods in asymmetric conjugate addition reactions have become dominant [2–4] chiral auxiliary mediated reactions are still employed to achieve the goal of diastereoselective bond formation [5–7]. Evans'oxazolidinones have proven to be the most versatile chiral auxiliaries for this process [8–15]. In this context, Mullins and coworkers were able to employ the Evans' auxiliary in an efficient synthesis of the individual enantiomers of Pilosinine (**3**) using an enantiodivergent process originating from a single chiral oxazolidinone [16]. In 2019, Ortiz and coworkers [17] were able to synthesize a series of γ -amino acids (**3**) by the application of the Evans' auxiliary in the asymmetric conjugate addition reactions in diastereoselectivities ranging from 96:4 to 98:2 (Scheme 1). In another recent example, Takayama and coworkers employed the Evans' oxazolidinone in the

synthesis of the *Lycopodium* alkaloid Lycopoclavamine-A (**8**) via an asymmetric conjugate addition (Scheme 1) [18]. The ratio of diastereomers that was obtained in the oxazolidinone directed conjugate addition was 94:6 favoring the desired isomer. The synthesis of this key fragment allowed Takayama and coworkers to complete the synthesis of their target with a key remote stereocenter set by the conjugate addition. Based on the success of the Evans' oxazolidinones as chiral auxiliaries in conjugate addition reactions, we became interested in exploring the application of 3,4,5,6-tetrahydro-2*H*-1,3,4-oxadiazin-2-ones (oxadiazinones, **9**) in these same reactions. Oxadiazinones are aza-homologs of the Evans' auxiliary and the additional nitrogen can be exploited as a stereochemical control element in asymmetric aldol addition reactions (Scheme 2) [19–24].

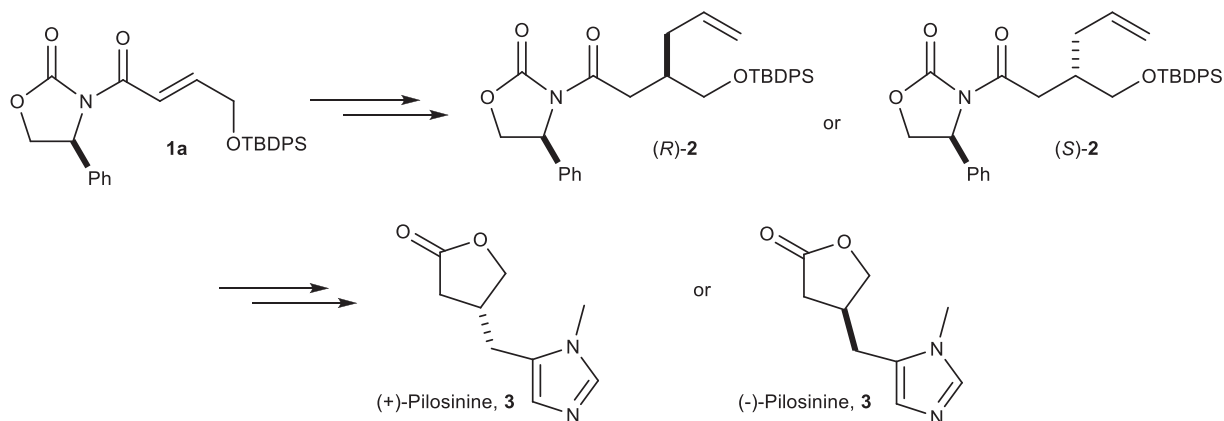
The asymmetric induction in these reactions is proposed to originate from the presence of the stereogenic *N*₄-nitrogen substituent. Based on this assessment, it was proposed that the oxadiazinones might be viable chiral auxiliaries for the process of asymmetric conjugate addition (Fig. 1). It was further proposed that a series of oxadiazinones could be prepared wherein the *N*₄-nitrogen position could be modified to have an increasing steric demand as a means of improving the level of diastereoselection. Thus, a series of oxadiazinones were prepared for this process and then

^{*} Corresponding author.

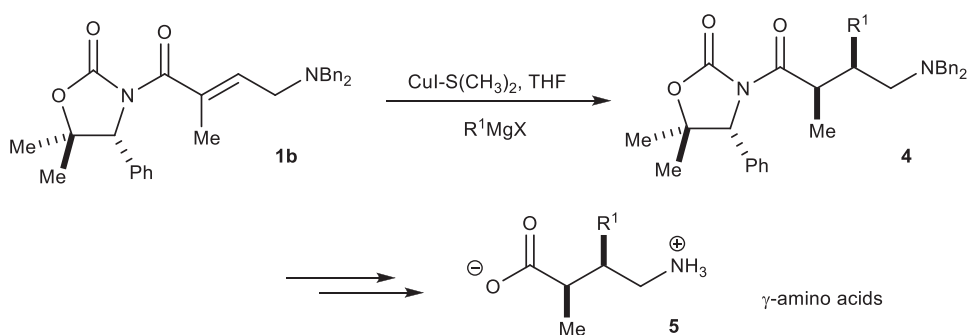
^{**} Corresponding author.

E-mail address: srhitch@ilstu.edu (S.R. Hitchcock).

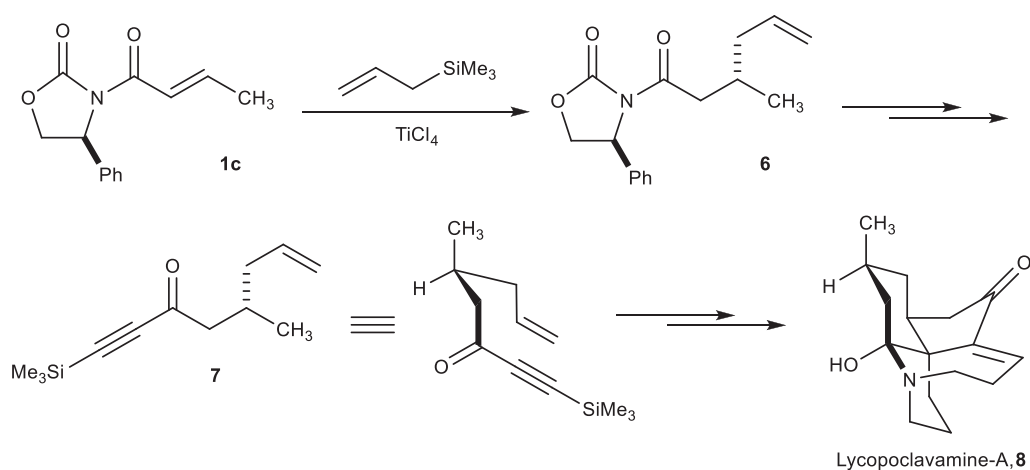
Mullins and coworkers



Ortiz and coworkers



Takayama and coworkers



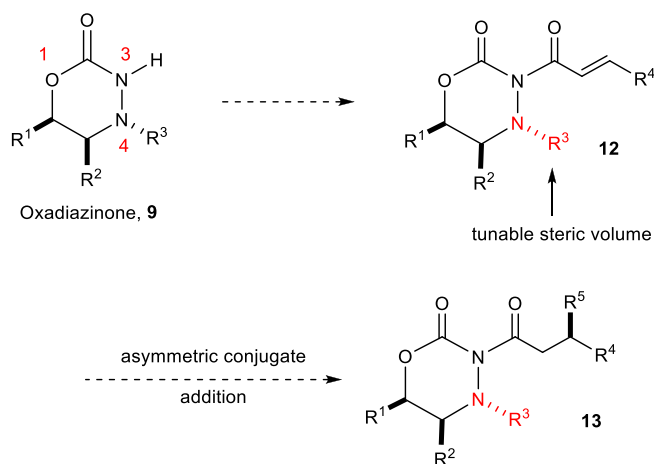
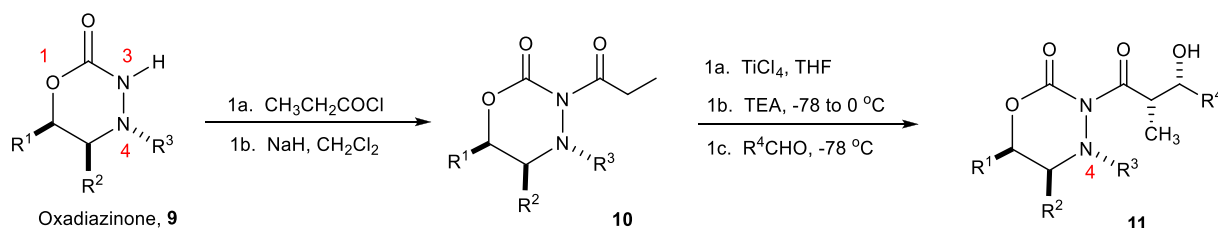
Scheme 1. Oxazolidinones as chiral auxiliaries in asymmetric conjugate addition.

tested in the process of conjugate addition.

2. Results and discussion

The (1*R*,2*S*)-ephedrine based oxadiazinone **9a** which had been initially employed in the asymmetric aldol addition reaction was prepared as previously described [24a]. This material was then

coupled with *trans*-cinnamic acid via the use of 1-ethyl-3-(3-dimethylamino propyl)carbodiimide (EDC) and DMAP in dichloromethane (Scheme 3). The N₄-*trans*-cinnamoyloxadiazinone was obtained in 71% isolated yield after chromatography. This product was then subjected to asymmetric conjugate addition reaction with methylmagnesium bromide and copper(I) bromide-dimethylsulfide complex at -78 °C. The addition product



was isolated as a 5:1 diastereomeric mixture of diastereomers as determined by integration of the well-resolved NMR spectral signals of the methyl group (diastereomer 1, $\delta = 0.59$ ppm; diastereomer 2, $\delta = 0.82$ ppm) of the appendant N_3 -acyl side chain. The diastereomeric products could not be readily separated by flash chromatography and the products were not crystalline so that single crystal X-ray crystallography was not a viable option. Thus, the absolute stereochemistry of the dominant stereoisomer was unambiguously determined by the coupling of the (1*R*,2*S*)-ephedrine based oxadiazinone with enantiomerically enriched (*S*)-3-phenylbutanoic acid using EDC and DMAP. Comparative analysis of the 500 MHz ^1H NMR spectrum of the crude conjugate addition product and the coupling reaction with the enantiomerically enriched 3-phenylbutanoic acid revealed that the diastereomer possessing the (*S*)-stereocenter for the conjugate addition was indeed the dominant diastereomer (Scheme 3).

There was a question of whether the application of different Grignard reagents to the oxadiazinone ring system via conjugate addition would yield improved results. Thus N_3 -crotonyl-oxadiazinone **14b** was prepared (LiH, *trans*-crotonoyl chloride) from **9a** and reacted with a series of Grignard reagents (EtMgBr, $\text{C}_6\text{H}_5\text{MgBr}$, and $p\text{-CH}_3\text{OC}_6\text{H}_4\text{MgBr}$) in the presence of copper(I) bromide dimethylsulfide complex. The diastereoselectivities ranged from 67:33 to 72:28 favoring the mode of stereochemical addition that was observed in the application of oxadiazinone **14b**.

This result of obtaining the (*S*)-conformation via the asymmetric conjugate addition was somewhat unexpected as the related Evans' oxazolidinones are known to predominantly form the product in which the addition pathway is the *anti*-addition (leading to *anti*-**18**) via the *syn-s-cis*-conformation of the acylated oxazolidinone system when Grignard reagents are used in conjunction with copper(I) reagents (Scheme 4). In this context, Schreiner, Bredenbeck and

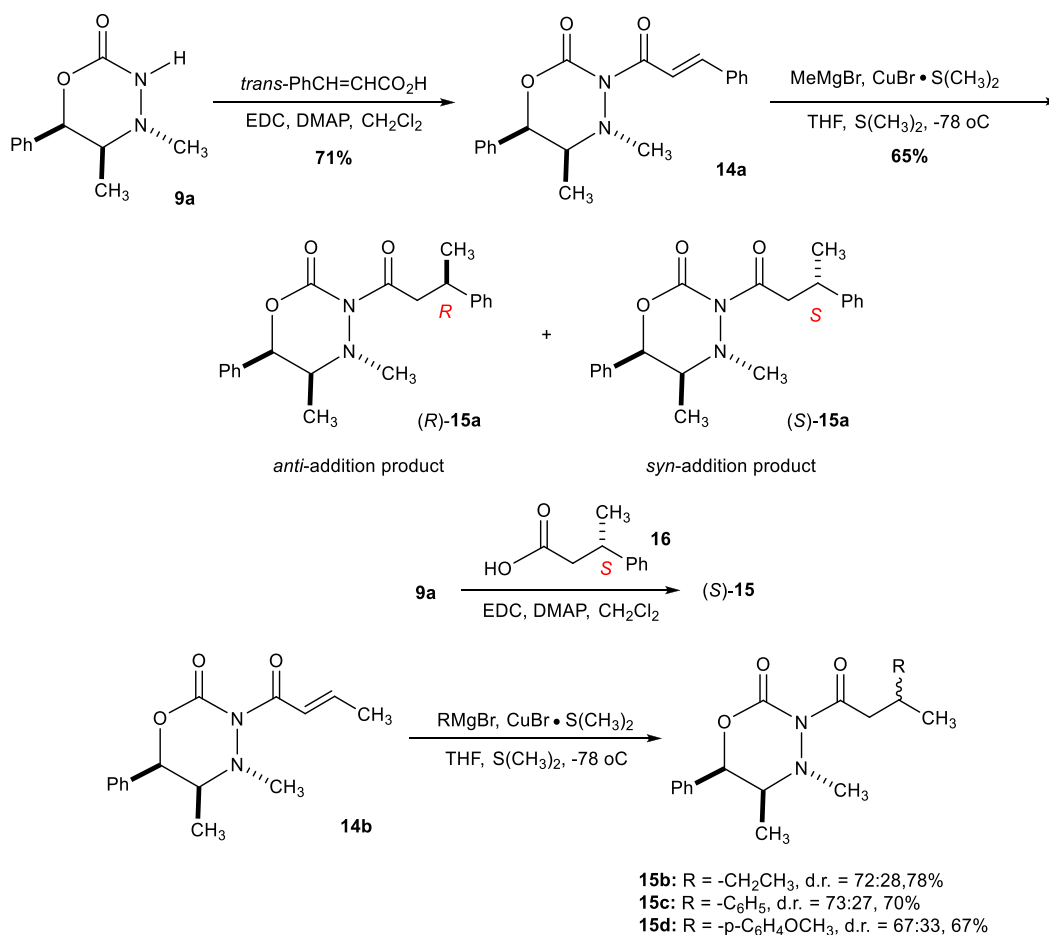
coworkers conducted solution studies using ultrafast two-dimensional infrared spectroscopy to suggest that the oxazolidinones adopt the coordinated *syn-s-cis*-**17** conformation during the course of coordination with magnesium salts [25]. The *anti-s-cis*-**17** conformation is also viable, but this conformation is more prevalent with use of alternate reagents [25]. The *syn-s-trans*-**17** and *anti-s-trans*-**17** conformations are not as populated due primarily to steric interactions.

Using the Evans' model of the asymmetric conjugate addition, the expected product would have been the *anti*-addition pathway leading to the formation of (*R*)-**15**. However, as described above, the product was unambiguously assigned as the *syn*-addition product (*S*)-**15**. This would suggest that either the *anti-s-cis*-**14a** conformer or the *syn-s-trans*-**14a** conformer or some combination thereof leads to the formation of the observed diastereomeric mixture of products that favor the predominant formation of the (*S*)-stereocenter (Scheme 5).

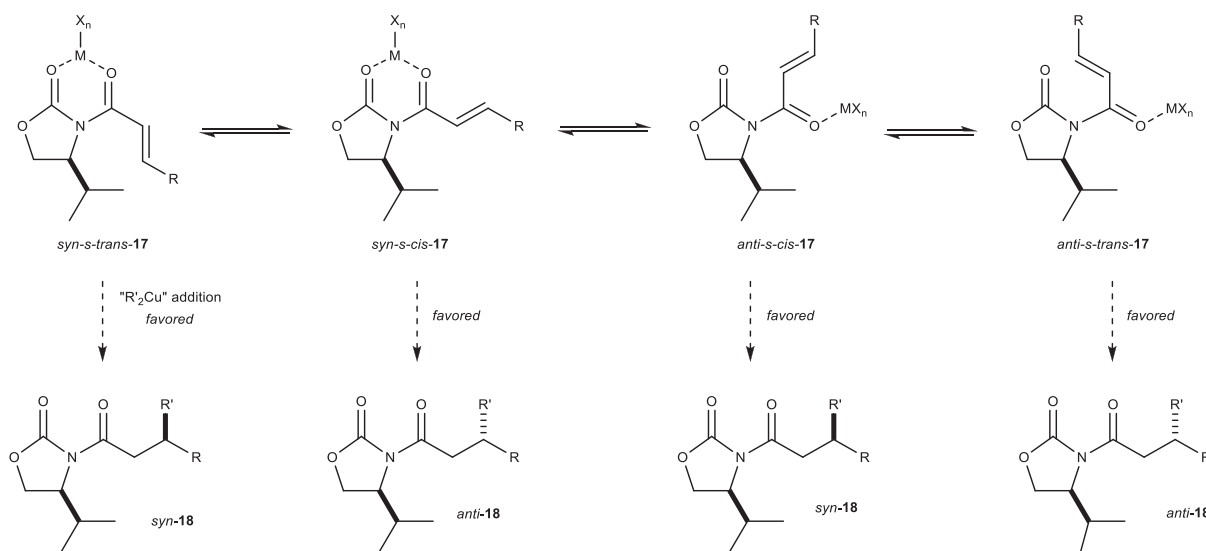
A NOESY spectrum of **14a** suggested that the *anti-s-cis*-conformation was the dominant form of the oxadiazinone as there was no observable NOE between the N_4 -methyl group and the β -proton of the N_3 -cinnamoyl side chain (Fig. 2). In addition to the solution state conformational analysis, an X-ray crystal structure was obtained for **14a** (Fig. 2). The crystal structure revealed in the solid state, that the carbonyl groups adopt an *anti*-conformation with a dihedral bond angle of -142.6° and the N_3 -cinnamoyl side-chain retained its *s-cis* conformation. It is noted that while the X-ray crystal structure is in agreement with the conformation suggested by the NOE experiment, it is a reflection of the dominant conformation in the solid state and may be the result of crystal packing forces.

A conformational study was conducted involving the proposed conformations of oxadiazinone **14a**. Initial structures were generated using the MMFF94 molecular mechanics force field [26] within the GMMX conformational searching facility of the GaussView 6.1 software package [27]. Over 50 potential conformers were then optimized at the $\omega\text{b97x-D/6-311++G(d,p)}$ level of theory in the gas phase and in solution using the Polarizable Continuum Model (PCM) for solvation with a dielectric constant corresponding to chloroform. The Gaussian 09 software package [28] was utilized for all the gas and solution phase density functional theory calculations.

The computational study revealed that the lowest energy conformer in the gas phase and the solution phase corresponded to an *anti-s-cis* conformation of oxadiazinone **14a**, in accord with the NOESY and X-ray crystal structure results; this finding holds for both the gas and solution phase results. The lowest energy conformers of each type (*anti-s-cis*, *anti-s-trans*, *syn-s-cis*, and *syn-s-trans*) of oxadiazinone **14a** are shown in Figs. 3 and 4 for the gas and solution phases, respectively, along with key dihedral angles defining the conformations. Table 1 presents the first 20 conformers found in the gas phase ordered in terms of total energy, while Table 2 provides a similar summary of the solution phase



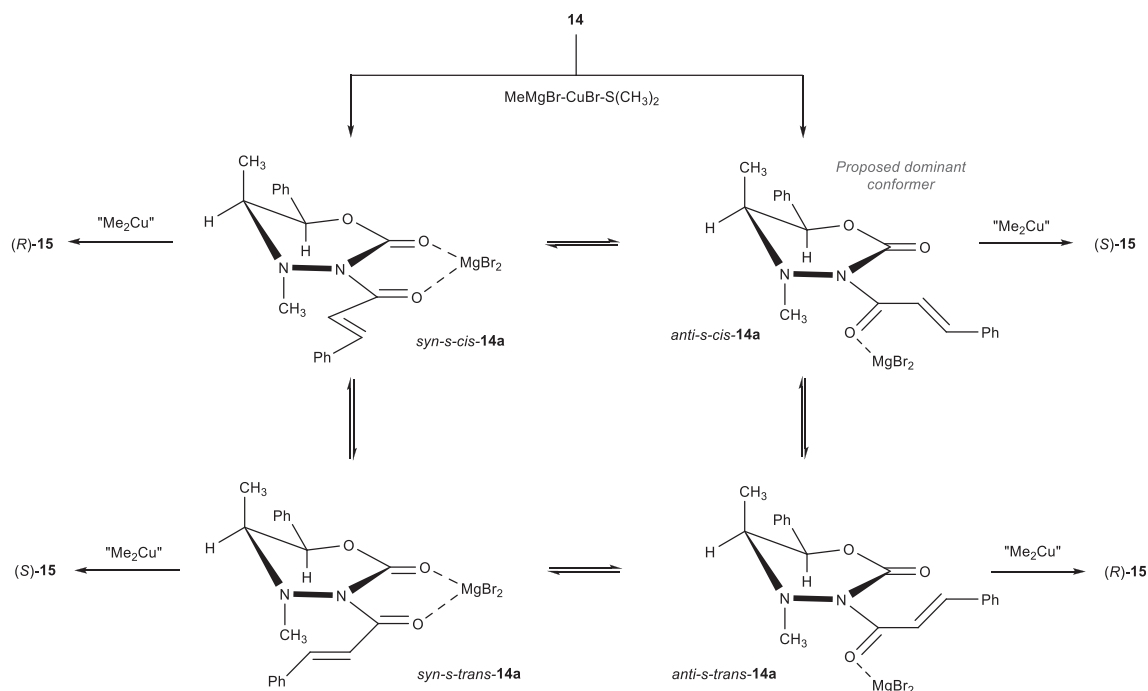
Scheme 3. Acylation and conjugate addition using oxadiazinone **9a**.



Scheme 4. Potential conformations for oxazolidinones in conjugate additions.

results. In addition, Table 1 provides the gas phase dipole moments of each of the conformers. Based on the collected results described in Tables 1 and 2, the ordering of the relative energies of the conformations is: *anti-s-cis* < *syn-s-cis* < *anti-s-trans* < *syn-s-trans*. In the gas phase, the separation in energy between the lowest *anti-s-*

cis and *syn-s-cis* conformers (Table 1, entries 1 and 2, respectively) is 2.4 kcal/mol, but drops to 0.6 kcal/mol in solution phase (Table 2, entries 1 and 2, respectively). This is a result of stabilization in polar solvent of the highly polar *syn-s-cis* conformation, which possesses a gas phase dipole moment of more than 7 Debye, much larger than



Scheme 5. Proposed mechanistic pathway of conjugate addition with oxadiazinone **14a**.

the dipole moments of the *anti*-conformations, which range from about 1 to 4 Debye. Similarly, the higher-energy *syn-s-trans* conformation (conformer 14 in the gas phase), with a gas phase dipole moment of 8.0 Debye, is significantly stabilized in solution relative to the *anti*-conformations and drops in energy from 8.0 kcal/mol in the gas phase to 5.1 kcal/mol in solution.

Two of the key geometrical parameters describing the orientation of oxadiazinone **14a** include the O25–C2–C15–O24 dihedral angle (which will be referred to as O=C–N–C=O) using the X-ray crystal structure numbering. For the lowest energy conformer of each type, these dihedral angles change only a small amount in solution phase relative to the gas phase values, as illustrated in Figs. 3 and 4. For the lowest energy *anti-s-cis* conformer in gas and solution phases (conformer 1 in both cases), the carbonyl groups deviate from the ideal anti-parallel orientation of $\pm 180^\circ$, with O=C–N–C=O dihedrals in the range of -142 to -146° . Similarly, the lowest energy *syn-s-cis* conformer in gas and solution phases (conformer 2 in both cases) exhibit O=C–N–C=O dihedral angles that deviate from the ideal parallel carbonyl orientation of 0° , with dihedrals in the range 26 – 31° . The conformations that tend to be higher in energy, *anti-s-trans* and *syn-s-trans*, exhibit O=C–N–C=O dihedral angles that show even greater deviations from the expected ideal O=C–N–C=O orientations ($\pm 180^\circ$). Deviations from the ideal dihedral angles for the lowest energy structures of the *anti-s-trans* and *syn-s-trans* conformations are as large as 61° for the O=C–N–C=O dihedral angle. These larger deviations are reflective of more strain in the *anti-s-trans* and *syn-s-trans* conformations, resulting in higher relative energies overall.

While these conformational studies provided a foundation of a potential rationale for the observed stereochemical outcome (Scheme 3), there was an interest in further evaluating the conjugate addition with oxadiazinone **14a** in greater detail with the putative coordinating MgBr₂ derived from the Grignard reagent combined with copper(I) bromide-dimethyl sulfide complex. Thus, the lowest-energy solution phase *anti-s-cis-14a* and *syn-s-cis-14a* conformers were allowed to coordinate with MgBr₂ (Fig. 5) and the resulting structures were optimized at the B3LYP/6-31G(d) level

using the PCM solvation model for chloroform as described previously.

It was observed that although the *anti-s-cis-14a* conformation is lowest in energy in the gas and solution phases by a small amount (0.6–2.4 kcal/mol) when un-complexed, the *syn-s-cis-14a* conformation corresponds to the lowest energy structure when interacting with MgBr₂. The extra lowering in the energy for the *syn* conformation comes as a result of the coordination of the magnesium to both carbonyl groups (Fig. 5).

Additional stabilization was also observed for *anti-s-cis-14a*-MgBr₂ due to interaction of the magnesium with the nearby N₄-nitrogen atom, although there is a longer magnesium-nitrogen bond of 2.40 Å. Natural Bond Orbital (NBO) analysis [29] was employed to confirm the interaction between the N₄-nitrogen and magnesium. Using NBO deletion analysis, the energy stabilization of *anti-s-cis-14a* due to the N₄-Mg interaction was found to be 8.6 kcal/mol. In comparing these two structures, the *syn-s-cis-14a*-MgBr₂ conformation is more stable than the *anti-s-cis-14a*-MgBr₂ conformation by 6.9 kcal/mol.

Despite the higher stability of the *syn-s-cis-14a*-MgBr₂ conformation, it is proposed that the *anti-s-cis-14a*-MgBr₂ conformer is more readily formed from the calculated initial conformation of the un-complexed *anti-s-cis-14a* because there is no need for a conformation change for complexation (the energetic cost for conversion from *anti-s-cis* to *syn-s-cis* via transition state in solution was calculated to be 6.7 kcal/mol at the B3LYP/6-31G(d) level, which is nearly the difference in energy between the two conformers). Thus, if the *anti-s-cis* conformation for **14a** is the dominant conformational form in solution, and if it is retained in the course of the conjugate addition, then a *Re*-face attack would be the preferred reaction pathway, and this would lead to the formation of the observed (*S*)-stereocenter (Scheme 6).

In order to further study the chemical behavior of the oxadiazinones in the asymmetric conjugate addition reaction, (1*S*,2*S*)-pseudoephedrine was employed. The (1*S*,2*S*)-pseudo ephedrine oxadiazinone was prepared as previously described [24b]. The oxadiazinone was coupled with *trans*-cinnamic acid to afford the

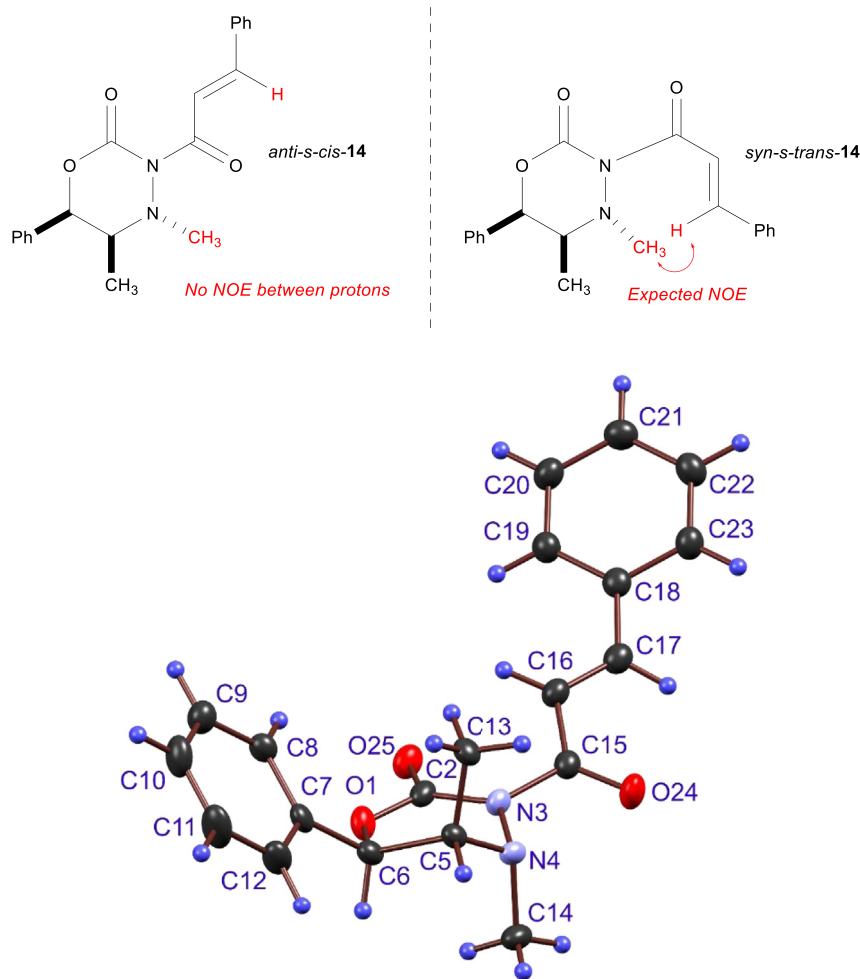


Fig. 2. NOESY study and X-ray crystal structure of oxadiazinone **14a**.

N_3 -*trans*-cinnamoyl derivative **18** in 59% isolated yield (Scheme 7). In contrast to the diastereomeric (1*R*,2*S*)-ephedrine based oxadiazinone **14a**, this oxadiazinone exhibited pyramidal inversion at the N_4 -nitrogen that was evident from line broadening observed in the 125 MHz ^{13}C NMR spectrum of **18** at the N_4 - and C_5 -positions (Fig. 6). Such conformational motion had been previously reported by our research group; variable temperature studies in the earlier study suggested that pyramidal inversion was the key mode of dynamic motion [24b]. Attempts to conduct conjugate addition reactions with **19** led to the formation of (*R/S*)-**20** as a mixture of diastereomers that could not be evaluated due to line broadening. Attempts to conduct an acid catalyzed hydrolysis to recover the 3-phenylbutyric acid hydrolysis product were also met with failure. At this stage, it was apparent that the pseudoephedrine based system would not be a viable candidate for the asymmetric conjugate addition.

In an effort to improve the level of diastereoselection in the oxadiazinone mediated asymmetric conjugate addition, an alternate oxadiazinone structure was pursued. The use of a (1*R*,2*S*)-norephedrine based N_4 -*p*-methoxybenzyl- N_3 -propanoyloxadiazinone **23** had been successfully employed in the asymmetric aldol addition reaction with a variety of aldehydes to yield diastereoselectivities ranging from 85:15 to 95:5 (Scheme 8).

It was reasoned that the increased steric volume of the N_4 -*p*-methoxybenzyl group would offer an improved diastereoselectivity in the conjugate addition reaction. To this end, oxadiazinone **24** was

prepared as previously described [19]. This oxadiazinone was acylated with *trans*-cinnamic acid using a carbodiimide approach employing EDC and DMAP to yield the N_3 -*trans*-cinnamoyloxadiazinone **25** ($R = \text{Ph}$ -) in 80% isolated yield after flash chromatography.

In a similar fashion, oxadiazinone **24** was treated with sodium hydride and acylated with *trans*-crotonoyl chloride to yield the N_3 -*trans*-crotonoyloxadiazinone **26** ($R = -\text{CH}_3$) in 51% isolated yield. Oxadiazinone **25** was then subjected to the conjugate addition reaction by treatment with methylmagnesium bromide and copper(I) bromide dimethylsulfide complex to yield a 3:1 ratio of diastereomers in 60% yield as illustrated in Scheme 8. The diastereomeric ratio was determined from the well-resolved doublets associated with the methyl group of the N_3 -side chain appearing at 0.58 ppm and 0.72 ppm.

There was an interest in determining the ratio of diastereomers in the opposing structural case in which the N_3 -substituent was a crotonoyl group (oxadiazinone **26**) and the added Grignard reagent was phenylmagnesium bromide (Scheme 8). The end result was that the observed level of diastereoselection was the same as it had been when the N_3 -substituent was a *trans*-cinnamoyl group and the added Grignard reagent was methylmagnesium bromide, i.e. 3:1. This finding suggested that the size of the Grignard reagent did not have a direct impact on the level of diastereoselection. Moreover, this observation reinforced the fact that the diastereoselectivity of the conjugate addition had been better in the case of the (1*R*,2*S*)-

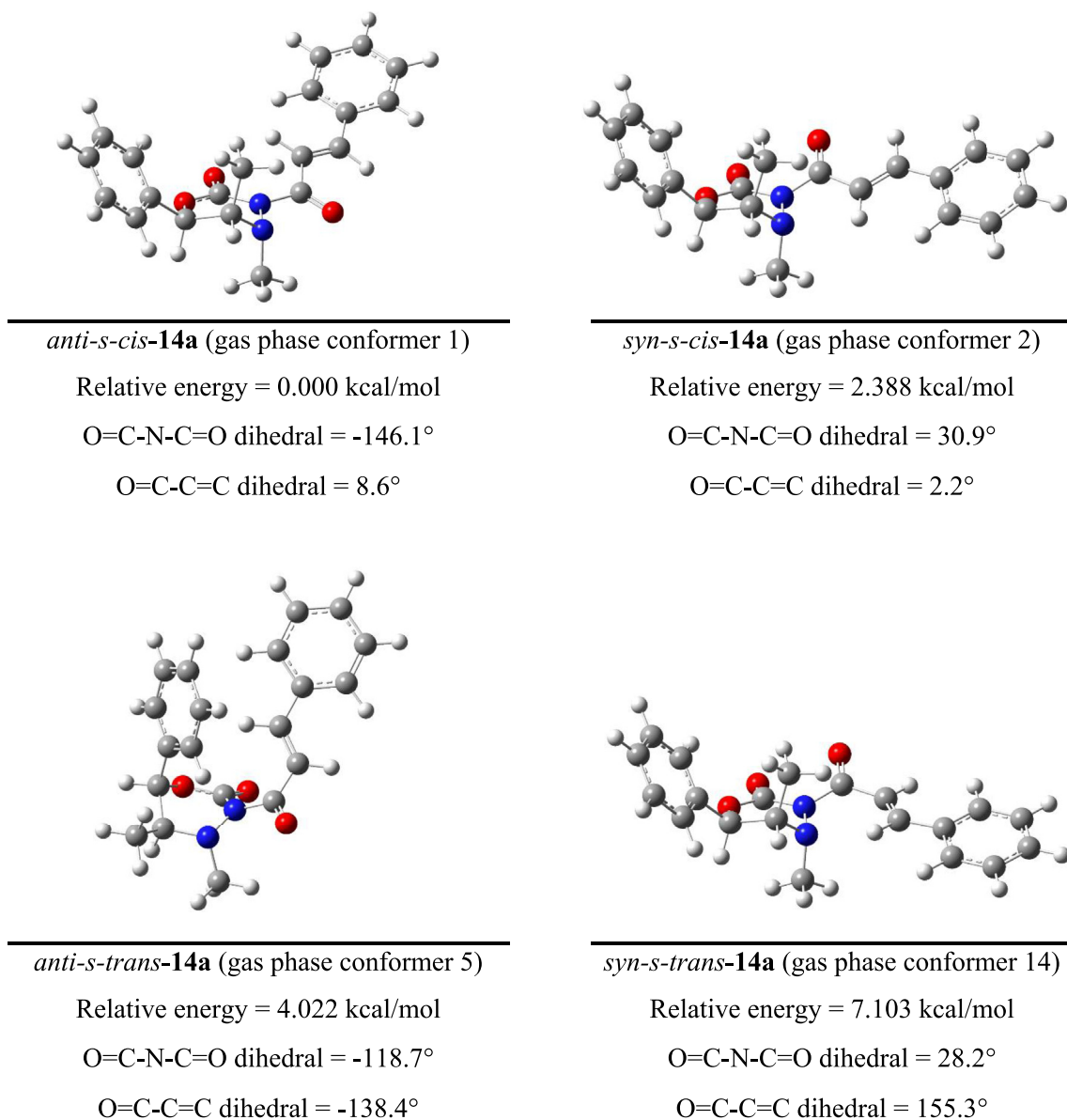


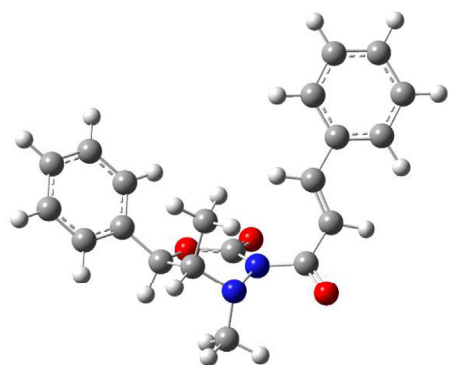
Fig. 3. Lowest energy gas phase conformers of oxadiazinone **14a**, ω b97x-D/6-311++G(d,p) level. The O=C-N-C=O dihedral angle corresponds to O25-C2-C15-O24 and the O=C-C=C dihedral angle corresponds to O24-C15-C16-C17, using the X-ray crystal structure numbering.

ephedrine based oxadiazinone where the diastereoselectivity was measured to be 5:1.

In the context of the stereochemical mode of addition, the (1*R*,2*S*)-ephedrine based oxadiazinone **15a** was determined to have had the (*S*)-conformation at the newly formed stereocenter. This was also determined to be the case for the (1*R*,2*S*)-norephedrine based oxadiazinone **26** through a process of oxidative cleavage of the *N*₃-side chain (Scheme 9). Analysis of the recovered 3-phenylbutyric acid revealed an optical activity of $[\alpha]_{\text{D}} = +22$ (*c* = 1, benzene); lit. = $[\alpha]_{\text{D}} = +57$ (*c* = 1, benzene) [30]. This data suggested that the stereochemical mode of the conjugate addition favored the formation of the (*S*)-configuration.

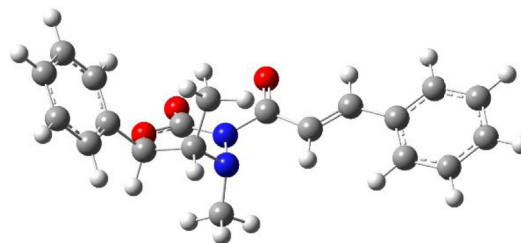
This result was surprising as it was expected that the increased steric volume of the *N*₄-*p*-methoxybenzyl group would have led to improved diastereoselection. A further investigation was pursued in which the *N*₄-substituent was further increased in its steric volume. It was reasoned that while the *N*₄-*p*-methoxybenzyl was

considerable in its steric demand, it was still considered to be a primary substituent. Thus, a secondary substituent was proposed as a means of probing the cause of the lower diastereoselectivity with the *N*₄-*p*-methoxybenzyl system and a potential means of increasing the diastereoselection in the oxadiazinone mediated conjugate addition reaction. To this end, (1*R*,2*S*)-norephedrine was used to create the *N*₄-isopropylloxadiazinone (**30**) as previously described [23]. This oxadiazinone was acylated by treatment with lithium hydride and *trans*-cinnamoyl chloride to yield the corresponding *N*₃-acylated derivatives **31** in 95% (Scheme 10). This substrate was then employed in the asymmetric conjugate addition using copper(I) bromide-dimethyl sulfide complex and methylmagnesium bromide to yield **32**. The level of diastereoselectivity that was observed was comparable to that of the instances in which the *N*₄-*p*-methoxybenzylloxadiazinone substrates **24** and **25** were employed, namely a 3:1 ratio of diastereomers. Based on this assessment, the mode of the stereochemical addition for **32** was

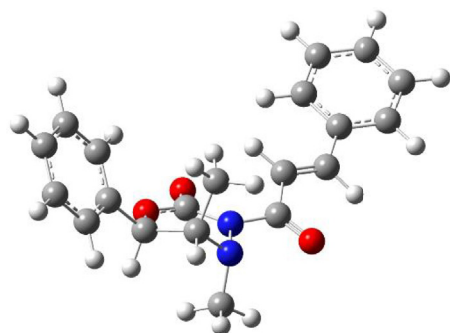
*anti-s-cis-14a* (solution phase conformer

1)

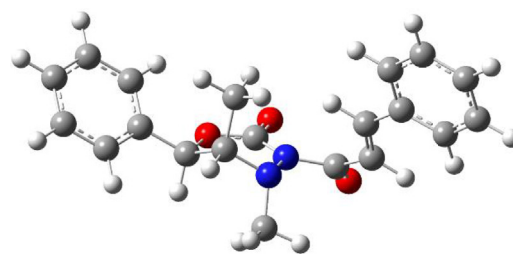
Relative energy = 0.000 kcal/mol

O=C-N-C=O dihedral = -141.3° O=C-C=C dihedral = 10.8° *syn-s-cis-14a* (solution phase conformer 2)

Relative energy = 0.598 kcal/mol

O=C-N-C=O dihedral = 25.7° O=C-C=C dihedral = 4.9° *anti-s-trans-14a* (solution phase conformer 5)

Relative energy = 3.508 kcal/mol

O=C-N-C=O dihedral = -121.2° O=C-C=C dihedral = -142.9° *syn-s-trans-14a* (solution phase conformer 10)

Relative energy = 5.137 kcal/mol

O=C-N-C=O dihedral = -42.3° O=C-C=C dihedral = 149.7°

Fig. 4. Lowest energy solution phase conformers for each conformation of oxadiazinone **14a**, ω b97x-D/6-311++G(d,p) level. The O=C-N-C=O dihedral angle corresponds to O25-C2-C15-O24 and the O=C-C=C dihedral angle corresponds to O24-C15-C16-C17, using the X-ray crystal structure numbering.

taken be the same as with substrates **24** and **25** by analogy.

The collected results suggested that the introduction of N_4 -substituents to the oxadiazinone larger than the N_4 -methyl substituent (oxadiazinone **14a**) would not have yielded an improved level of diastereoselection. In fact, the use of the more sterically demanding N_4 -isopropyl substituent of oxadiazinone **31** versus that of the N_4 -methyl group of oxadiazinone **14a** caused the diastereoselection to decrease from a 5:1 ratio to a 3:1 ratio. The computational study concerning the conformation dynamics of the un-complexed-**14a** and MgBr_2 -complexed-**14a** suggested that the stereochemical course of the reaction was heavily influenced by the *anti-s-cis-14a*- MgBr_2 intermediate (Scheme 6, *vide supra*). By analogy, it was proposed that the N_4 -isopropoxyoxadiazinone **31** might follow a similar route as depicted in Scheme 11. Based on this proposal, the N_4 -isopropoxyoxadiazinone would have yielded an improved diastereoselection via the *anti-s-cis-31*- MgBr_2

intermediate but this was not observed.

A computational study of N_4 -isopropyl-substituted system was conducted in a similar fashion to that of oxadiazinone **14a**. Initial structures were generated using the MMFF94 molecular mechanics force field [26] within the GMMX facility of the GaussView 6.1 software package [27]. The 80 lowest energy conformers from the MMFF94 conformation search were then optimized in gas and solution phase using the B3LYP/6-31G(d) level of theory. Finally, the lowest 25 conformers from the B3LYP/6-31G(d) level were then re-optimized at the ω b97x-D/6-311++G(d,p) level in the gas phase and in solution using the Polarizable Continuum Model (PCM) for solvation with a dielectric constant corresponding to chloroform. The Gaussian 09 software package [28] was utilized for all the gas and solution phase density functional theory calculations.

For the N_4 -isopropyl-substituted oxadiazinone **31**, the lowest energy conformer is different in the gas phase and in solution

Table 1

Results for the first 20 conformers of oxadiazinone **14a**, found in the gas phase at the ω b97x-D/6-311++G(d,p) level of theory. The lowest energy conformer of each type is highlighted in gray.

Conformer entry	Classification	Relative E (kcal/mol)	Dipole Moment (Debye)
1	<i>anti-s-cis</i>	0.000	2.939
2	<i>syn-s-cis</i>	2.388	7.503
3	<i>anti-s-cis</i>	2.905	3.003
4	<i>anti-s-cis</i>	3.754	3.064
5	<i>anti-s-trans</i>	4.022	4.075
6	<i>anti-s-trans</i>	4.086	4.247
7	<i>anti-s-trans</i>	4.468	3.501
8	<i>anti-s-cis</i>	5.104	2.373
9	<i>anti-s-cis</i>	5.307	2.542
10	<i>syn-s-cis</i>	5.622	7.733
11	<i>anti-s-cis</i>	5.824	2.409
12	<i>syn-s-cis</i>	5.965	7.280
13	<i>anti-s-cis</i>	5.984	2.612
14	<i>syn-s-trans</i>	7.103	8.009
15	<i>syn-s-trans</i>	7.401	7.962
16	<i>anti-s-trans</i>	7.484	4.272
17	<i>anti-s-trans</i>	8.378	2.543
18	<i>anti-s-trans</i>	8.422	2.598
19	<i>anti-s-trans</i>	8.537	3.008
20	<i>anti-s-trans</i>	8.798	1.170

Table 2

Results for the first 20 conformers of oxadiazinone **14a** found in solution phase (chloroform) at the ω b97x-D/6-311++G(d,p) level of theory. The lowest energy conformer of each type is highlighted in gray.

Conformer entry	Classification	Relative E (kcal/mol)
1	<i>anti-s-cis</i>	0.000
2	<i>syn-s-cis</i>	0.598
3	<i>syn-s-cis</i>	1.066
4	<i>anti-s-cis</i>	3.141
5	<i>anti-s-trans</i>	3.508
6	<i>anti-s-cis</i>	3.743
7	<i>syn-s-cis</i>	3.840
8	<i>anti-s-trans</i>	4.019
9	<i>syn-s-cis</i>	4.260
10	<i>syn-s-trans</i>	5.137
11	<i>anti-s-cis</i>	6.113
12	<i>anti-s-cis</i>	6.285
13	<i>anti-s-cis</i>	6.585
14	<i>anti-s-trans</i>	6.613
15	<i>anti-s-cis</i>	7.149
16	<i>anti-s-trans</i>	7.657
17	<i>syn-s-trans</i>	8.222
18	<i>anti-s-trans</i>	8.569
19	<i>anti-s-trans</i>	8.916
20	<i>anti-s-trans</i>	9.888

phase; this is in contrast to the N_4 -methyloxadiazinone **14a**, for which the lowest energy conformer corresponds to the *anti-s-cis* conformation in both the gas and solution phases. In the gas phase, the lowest energy conformer of N_4 -isopropyl-substituted oxadiazinone **31** is the *anti-s-cis* conformation (Fig. 7); however, in solution phase, the lowest energy conformer of **31** corresponds to the *syn-s-cis* conformation (Fig. 8). Table 3 lists the first 25 conformers found in the gas phase, and Table 4 presents the solution phase results. The lowest energy conformers for each conformation of the isopropyl-substituted oxadiazinone **31** are shown in Figs. 7 and 8 for the gas and solution phases, respectively, along with key dihedral angles.

In the gas phase, the energy ordering of the lowest energy conformation for each conformation of **31**, shown in Table 3, is: *anti-s-cis* < *syn-s-cis* < *anti-s-trans* < *syn-s-trans*. In contrast, the

energy ordering in solution phase of the lowest energy conformation for each conformation of isopropyl-substituted oxadiazinone **31**, shown in Table 4, is: *syn-s-cis* < *anti-s-cis* < *anti-s-trans* < *syn-s-trans*. The energy separation between the lowest *anti-s-cis* and *syn-s-cis* conformers is 0.8 kcal/mol in the gas phase, with the *anti-s-cis* conformation lower. This reverses in solution phase, with the *syn-s-cis* conformation lower by 1.0 kcal/mol. These results are consistent with the greater stabilization in polar solvent of the *syn-s-cis* conformation with its large gas phase dipole moment (7.6 Debye) relative to the *anti-s-cis* conformation with a dipole moment of 2.6 Debye. Similarly, the lowest *syn-s-trans* conformer, also with a dipole moment of more than 7 Debye, drops in energy from 7.8 kcal/mol in the gas phase to 6.3 kcal/mol in solution.

The changes in the key O=C–N–C=O and O=C–C=C dihedral angles in going from gas to solution phase are generally small, as indicated in Figs. 7 and 8. Variations overall are less than 20° and in most cases are less than 12°. For the N_4 -isopropyl-substituted oxadiazinone **31**, the lowest-energy conformations of the *anti-s-cis* and *syn-s-cis* conformations exhibit O=C–N–C=O dihedral angles that deviate by up to 36° from the ideal expected values of $\pm 180^\circ$ and 0° for the *anti* and *syn* conformations, respectively, in both gas and solution phases. The O=C–C=C dihedral angles for these conformations are within 15° of the expected 0° result for the *cis* orientation. The higher-energy conformations, *anti-s-trans* and *syn-s-trans*, show even greater deviations from ideal for the O=C–N–C=O and O=C–C=C dihedrals. Differences of up to 57° are observed for the O=C–N–C=O dihedral angles and deviations of up to 32° are observed for the O=C–C=C dihedral angles.

In comparing the lowest energy conformer of each type for N_4 -isopropyl oxadiazinone **31** with those of N_4 -methyloxadiazinone **14a**, it can be observed that the isopropyl substitution has little effect on the geometries of the lowest energy conformers of the *anti-s-cis-31* and *syn-s-cis-31* conformations. For these cases, the O=C–N–C=O and O=C–C=C dihedral angles of **31** are within 15° (and in most cases within 7°) of those for oxadiazinone **14a**. In contrast, the effect of isopropyl substitution is much more significant for the lowest energy conformers of *anti-s-trans-31* and *syn-s-trans-31*. For these cases, the O=C–N–C=O and O=C–C=C dihedral angles of the isopropyl-substituted compound can vary widely, with swings of up to nearly 180° in some cases.

With the conformational aspects of oxadiazinone **31** established, a series of computations were carried out in which **31** was complexed with MgBr₂ (Fig. 9). For the isopropyl-substituted oxadiazinone **31**, the interaction with MgBr₂ is similar to what was observed for oxadiazinone **14a**. As shown in Fig. 9, the *syn-s-cis* and *syn-s-trans* conformations of **31**-MgBr₂ are the lowest conformations as a result of the interaction of magnesium with both O25 and O24; however, the *syn-s-trans*-conformation lies more than 8 kcal/mol above the *syn-s-cis* conformation (compared with 6.4 kcal/mol for oxadiazinone **14a**).

Due to the presence of the bulkier isopropyl group attached to N_4 -nitrogen in oxadiazinone **31**, the *anti-s-trans* conformation with MgBr₂ does not exhibit any additional stabilization as a result of interaction of the magnesium with nitrogen N_4 ; the isopropyl group effectively blocks access to this interaction. Interestingly, this same *anti-s-trans-31* conformation in the un-complexed system is only 1 kcal/mol less stable than the *syn-s-cis* counterpart-**31**.

Based on the computational study on oxadiazinone **31** in its un-complexed form and complexed form with MgBr₂, it became clear that there were discrete conformational differences from oxadiazinone **14a**. These differences led to significant shifts in the conformational positioning of the N_3 -cinnamoyl side chain upon complexation, thereby leading to the different stereochemical outcomes for oxadiazinones **14a** (N_4 -methyl) and **31** (N_4 -isopropyl) (Fig. 10).

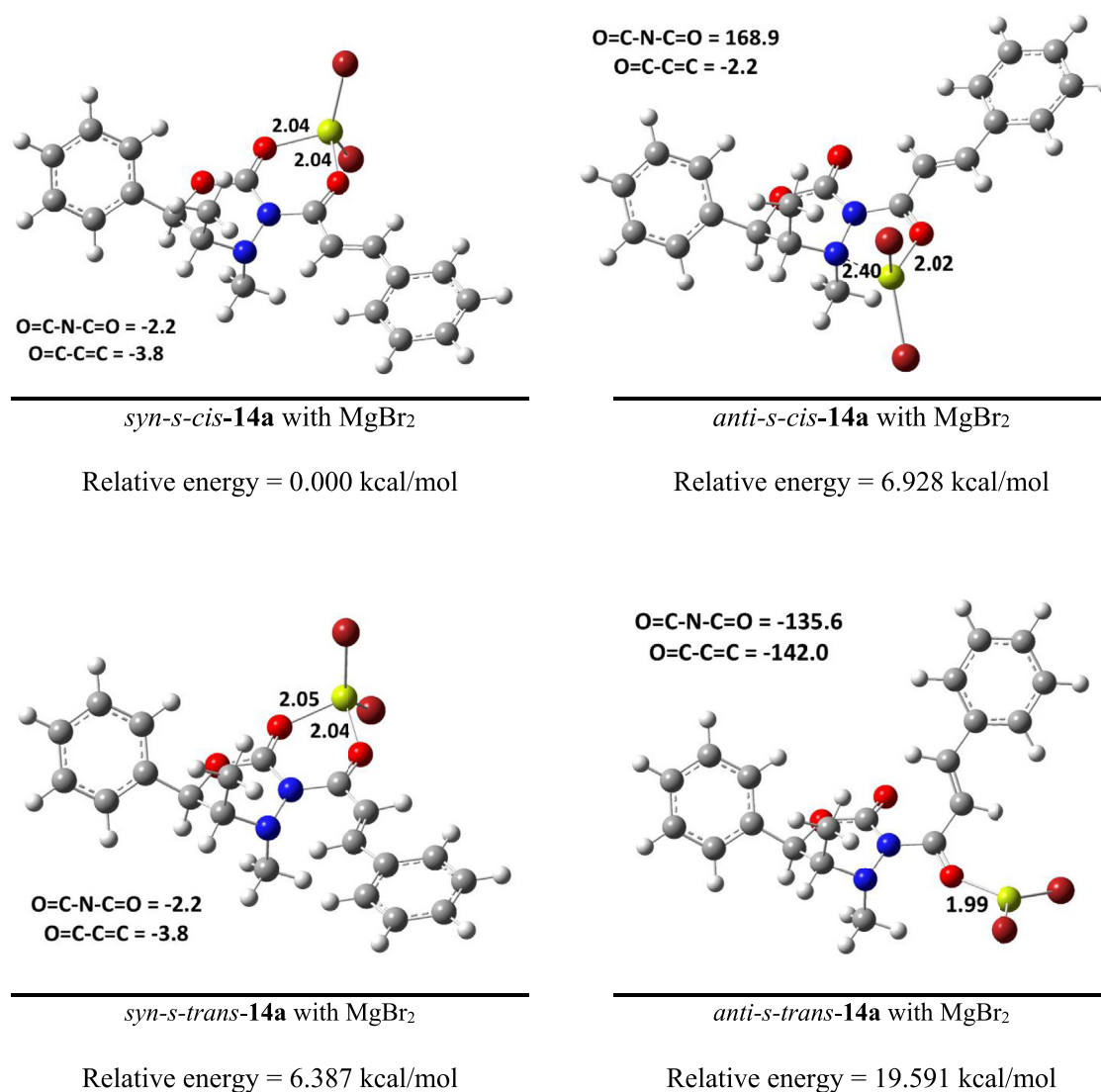


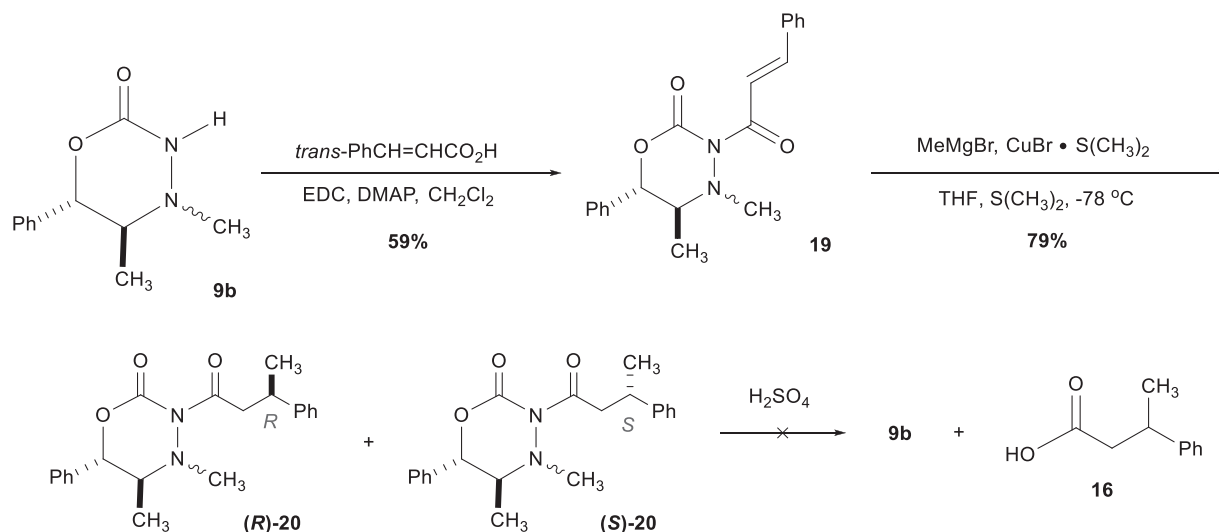
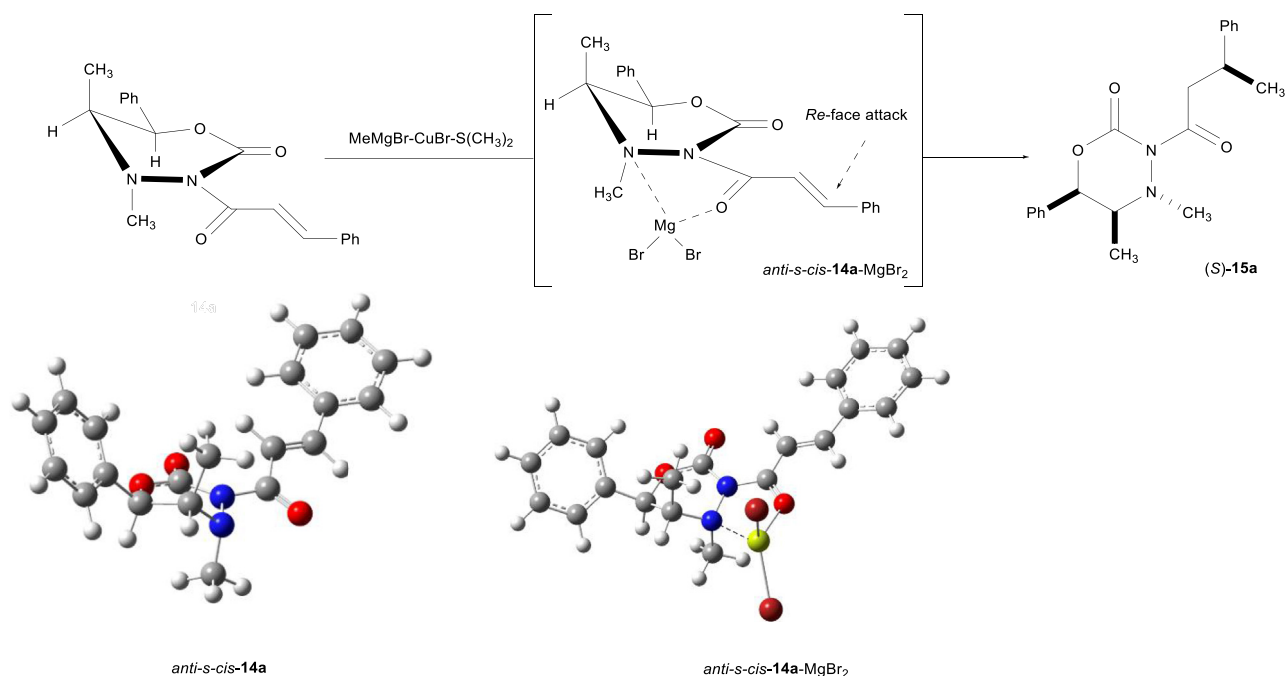
Fig. 5. Properties of structures obtained for the interaction of MgBr₂ with oxadiazinone **14a** in chloroform, determined at the B3LYP/6-31G(d) level. The O=C–N–C=O dihedral angle shown corresponds to O25–C2–C15–O24 and the O=C–C=C dihedral angle corresponds to O24–C15–C16–C17, using the X-ray crystal structure numbering.

It is proposed that the *anti-s-cis-31* and *syn-s-cis-31* conformations are present in solution along with other conformations that are non-ideal in terms of their geometries that lead to the stereochemical induction that was compromised as compared to the complexed *N*₄-methyloxadiazinone **14a**. Perhaps the most important difference established by the computational studies was that oxadiazinone **14a** possesses an *anti-s-cis*-conformation stabilized through coordination with the *N*₄-nitrogen of the ring system. In contrast, the complexed *N*₄-isopropoxyoxadiazinone **31** proved to be significantly higher in energy due to the steric volume of the *N*₄-isopropyl group. With this conformation destabilized, other conformations become viable options for the asymmetric conjugate addition leading to the compromised stereoselection.

3. Conclusion

A (1*R*,2*S*)-ephedrine based oxadiazinone and two (1*R*,2*S*)-nor-ephedrine based oxadiazinones were employed as chiral auxiliaries in the asymmetric conjugate addition reaction. The *N*₄-methyloxadiazinone **14a** yielded a diastereomeric ratio of 5:1 favoring the

formation of the (*S*)-conformation. The use of larger stereo-directing substituents (*N*₄ = -benzyl, **25**; *N*₄ = -isopropyl, **31**) to enhance the level of diastereoselection yielded compromised diastereoselectivities of 3:1. The lower diastereomeric ratio is attributed to the conformations present for the oxadiazinones. In this context, the computational conformational studies suggested that the *N*₄-methyloxadiazinone **14a** adopted an *anti-s-cis*-conformation which was in alignment with the observed solution phase conformation (NOE). In contrast, by way of the computational study, the *N*₄-isopropoxyoxadiazinone was found to have the *anti-s-cis*-conformation favored in the gas phase and the *syn-s-cis* conformation favored in the solution phase. In addition to this, the *N*₄-isopropoxyoxadiazinone was also found to have deviations in key bond angles in the lowest energy conformers that were not as prevalent in the *N*₄-methyloxadiazinone. With the experimental observations and the computational study, it is suggested that the conformational stability of the oxadiazinone in the asymmetric conjugate addition reaction is determined, in part, by the steric volume of the *N*₄-substituent. The smaller substituent in **14a** (*N*₄-methyl) yields a dominant conformation that readily undergoes the



conjugate addition, while a larger substituent, as in **25** (N_4 -benzyl) or **31** (N_4 -isopropyl) causes there to be multiple conformational intermediates that ultimately erode the level of diastereoselection.

4. Experimental

4.1. General information

Chemical reagents were used as purchased. Methyl sulfide was purchased as an anhydrous solution. All Grignard reagents were used as purchased and stoichiometric calculations were based on the stated concentration from the vendor. All reactions were conducted in flame-dried glassware under a dry nitrogen atmosphere. Crude reaction mixtures were purified by flash chromatography

using an automated flash chromatograph. The stationary phase was 40 g normal phase silica gel cartridges. The collected fractions were analyzed by thin layer chromatography with tlc plates coated with fluorescent indicator F₂₅₄ and visualized with UV light. All ¹H and ¹³C NMR spectra were recorded in deuterated chloroform (CDCl₃) using a Bruker Ultrashield Avance III NMR spectrometer operating at 500 MHz (or 400 MHz) for ¹H NMR spectra and operating at 125 MHz (or 100 MHz), respectively. Chemical shifts were reported in parts per million (δ scale) and coupling constant (J values) are listed in Hertz (Hz). Tetramethylsilane (TMS) was used as internal standard ($\delta = 0$ ppm). Infrared spectra were recorded using NaCl plates. Infrared spectral values were reported in reciprocal centimeters (cm^{-1}) and were measured as a neat liquid, nujol mull, or as a neat liquid film from an evaporated CDCl₃ solution. For

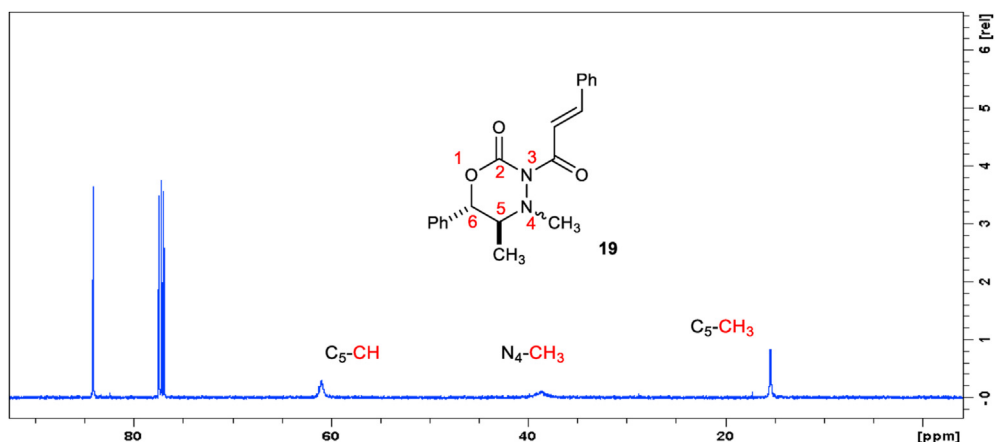
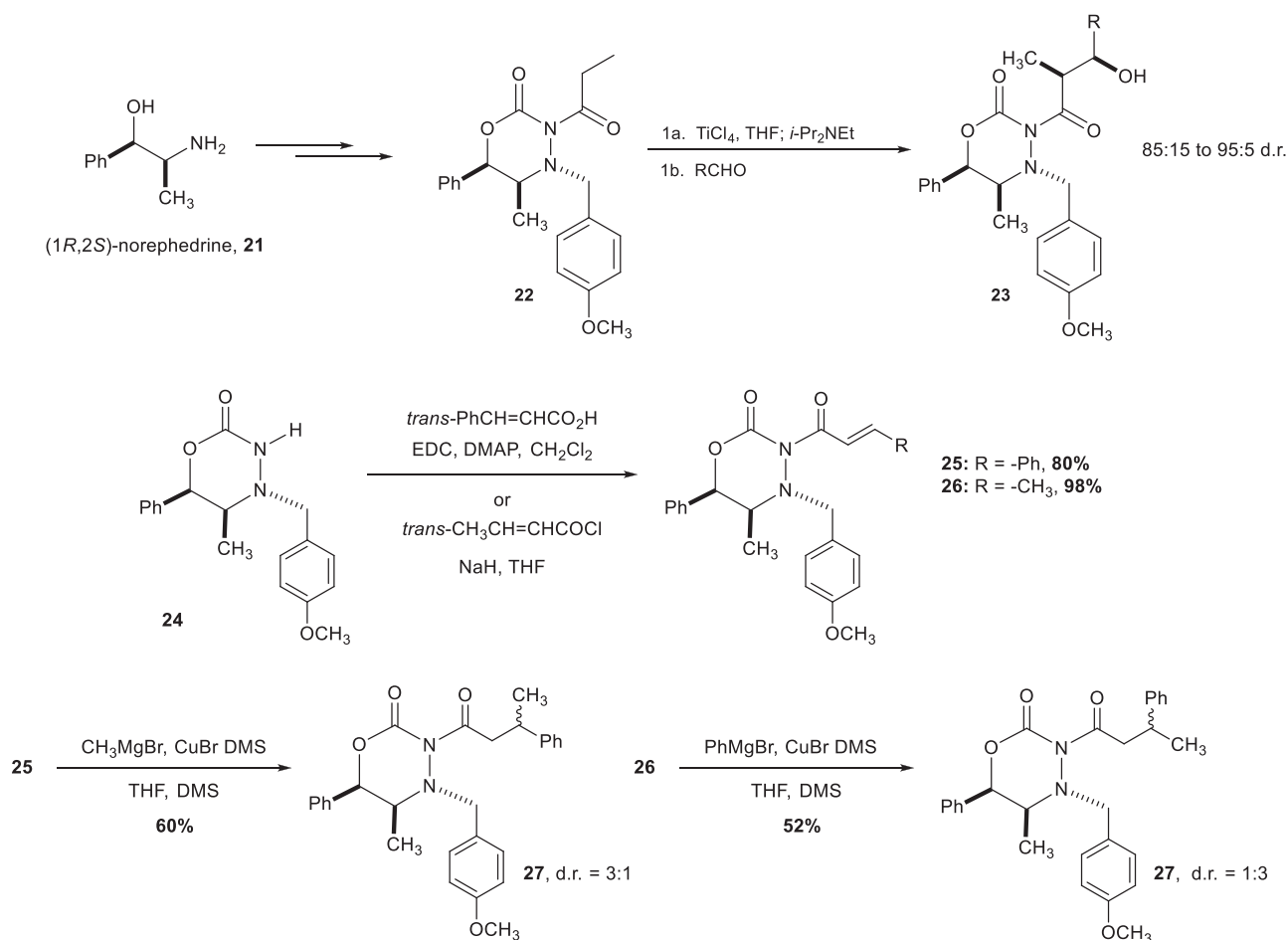


Fig. 6. Observable 125 MHz C-13 spectrum showing line broadening for oxadiazinone **19**.

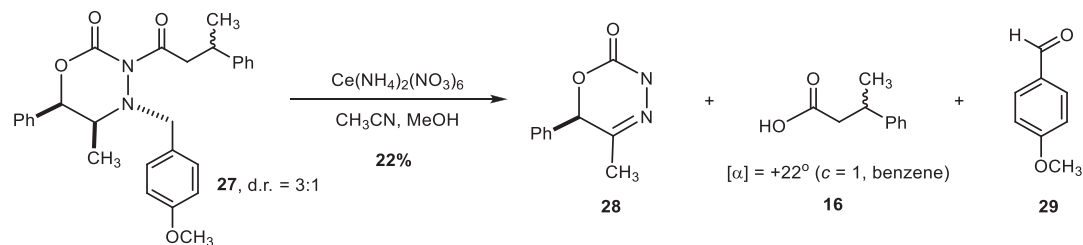


Scheme 8. Application of (1*R*,2*S*)-norephedrine based oxadiazinone **25** in the conjugate addition.

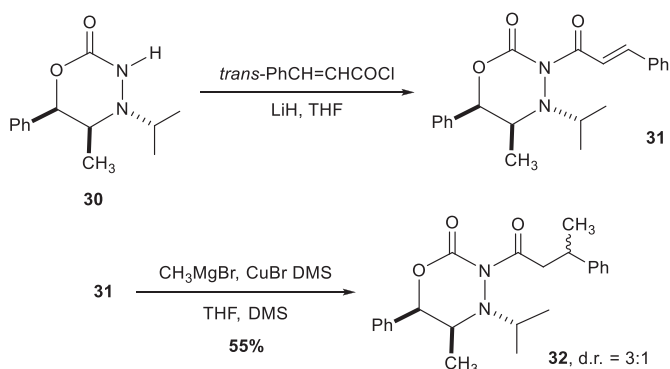
Electrospray Ionization High Resolution Mass Spectrometry (ESI-HRMS), samples were prepared in concentrations of 5–25 ppm in HPLC grade methanol/water/formic acid (1:1:0.01). Analytical data was collected using a ThermoScientific Q-Exactive ESI mass spectrometer.

4.2. (5*S*,6*R*)-3-*trans*-cinnamoyl-4,5-dimethyl-6-phenyl-1,3,4-oxadiazinone (**14a**)

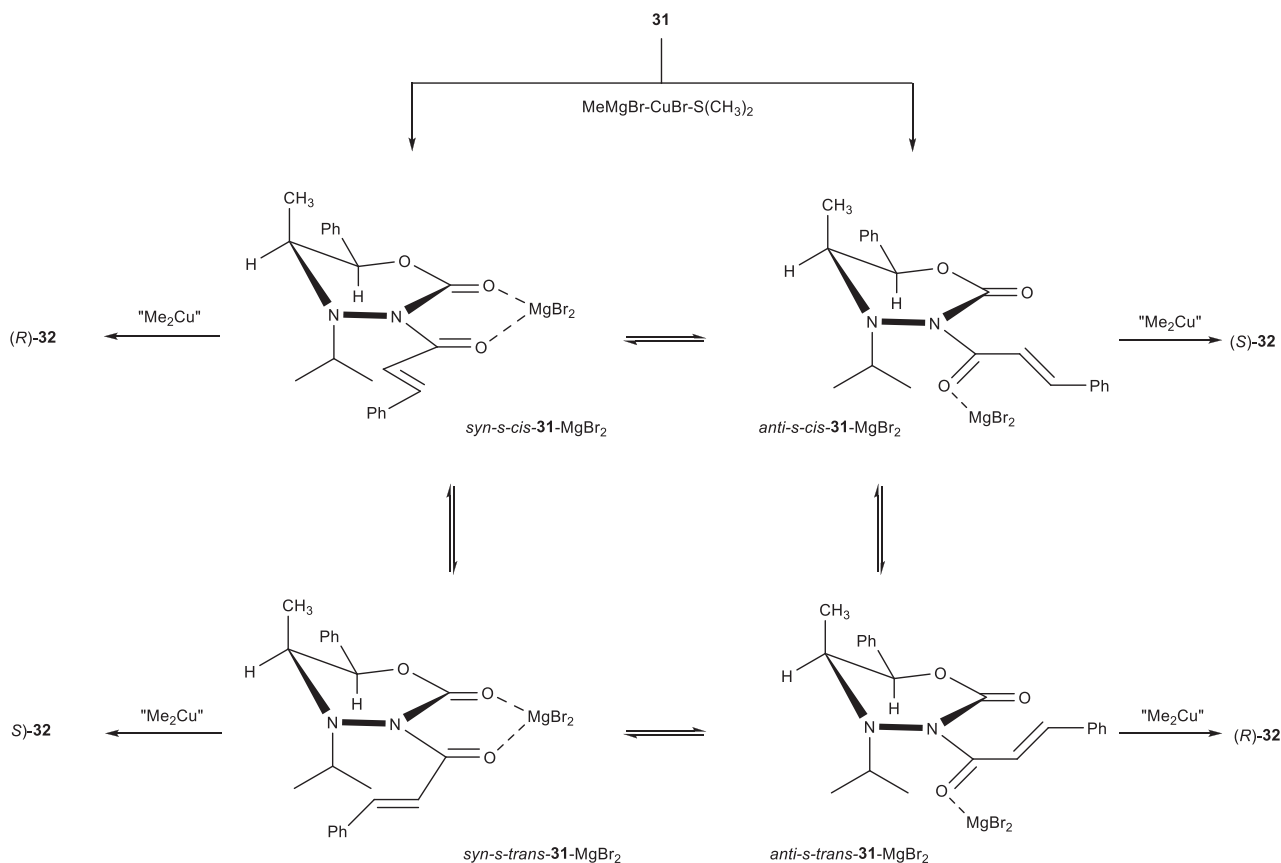
To a flame dried, nitrogen purged 250 mL round bottom flask was added *trans*-cinnamic acid (1.29 g, 8.72 mmol) and dissolved in anhydrous dichloromethane (16 mL). This was followed with the addition of the coupling agent 1-ethyl-3-(3-dimethylaminopropyl) carbodiimide (EDC) (1.671 g, 8.72 mmol), DMAP (0.134 g,

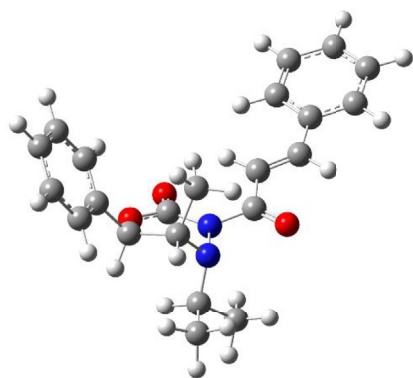


Scheme 9. Oxidative cleavage and stereochemical determination.

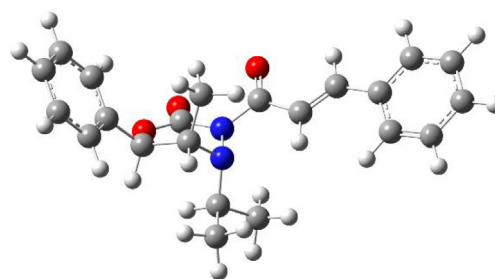
Scheme 10. Conjugate addition with the N_4 -isopropylloxadiazinone **31**.

1.09 mmol) and the oxadiazinone substrate (0.900 g, 4.36 mmol), sequentially and left stirring at room temperature for 16 h. The reaction was then diluted with dichloromethane (80 mL) and washed with 1 M HCl (20 mL), 1 M NaOH (2×20 mL) followed by brine (20 mL) wash. The organic layer thus recovered was dried (MgSO_4), gravity filtered, and the solvent removed under reduced pressure. The crude product was purified by flash column chromatography (hexanes:ethyl acetate, 70:30) to yield the title compound (1.034 g, 71%) as a white solid: *mp*: 125–128 °C. ^1H NMR (500 MHz, CDCl_3): δ 0.93 (d, $J = 7.0$ Hz, 3H), 3.08 (s, 3H), 3.48 (dq, $J = 6.9, 4.6$ Hz, 1H), 6.12 (d, $J = 4.6$ Hz, 1H), 7.34–7.38 (m, 3H), 7.41–7.45 (m, 5H), 7.61–7.64 (m, 3H), 7.88 (d, $J = 15.6$ Hz, 1H); ^{13}C NMR (125 MHz, CDCl_3): δ 12.7, 43.8, 56.9, 77.9, 119.0, 125.0, 128.2, 128.4, 128.7, 128.9, 130.5, 134.8, 135.8, 145.8, 148.1, 166.6; IR (CHCl_3): 1730, 1704, 1623, 1267, 1197, 724, 703 cm^{-1} . ESI HRMS for $\text{C}_{20}\text{H}_{20}\text{N}_2\text{NaO}_3^+$: calcd ($M + \text{Na}^+$) 359.1366, found 359.1366.

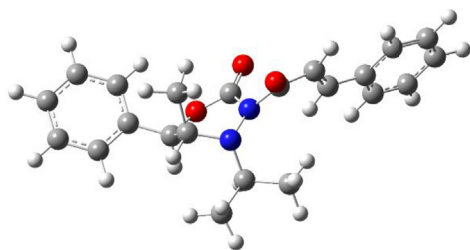
Scheme 11. Proposed mechanistic pathway of conjugate addition with oxadiazinone **31**.

*anti-s-cis-31* (gas phase conformer 1)

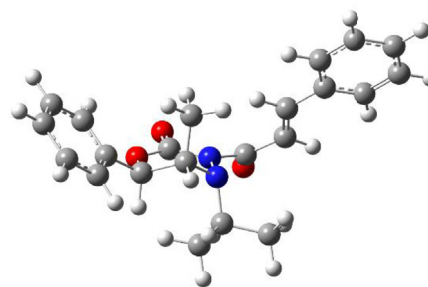
Relative energy = 0.000 kcal/mol

O=C-N-C=O dihedral = -158.7° O=C-C=C dihedral = 1.6° *syn-s-cis-31* (gas phase conformer 4)

Relative energy = 1.481 kcal/mol

O=C-N-C=O dihedral = 30.7° O=C-C=C dihedral = 2.2° *anti-s-trans-31* (gas phase conformer 11)

Relative energy = 3.817 kcal/mol

O=C-N-C=O dihedral = 124.1° O=C-C=C dihedral = 154.0° *syn-s-trans-31* (gas phase conformer 25)

Relative energy = 7.743 kcal/mol

O=C-N-C=O dihedral = -44.7° O=C-C=C dihedral = 151.9°

Fig. 7. Lowest energy gas phase conformers of isopropyl-substituted oxadiazinone **31**, ωb97x-D/6-311++G(d,p) level. The O=C-N-C=O dihedral angle corresponds to O25-C2-C15-O24 and the O=C-C=C dihedral angle corresponds to O24-C15-C16-C17.

4.3. (5*S*,6*R*)-4,5-dimethyl-6-phenyl-3-(3'-phenylbutanoyl)-1,3,4-oxadiazinone (**15a**)

To a 100 mL flame-dried, nitrogen-purged three-neck round bottomed flask fitted centrally with a 60 mL addition funnel was added copper bromide-dimethyl sulfide complex (0.933 g 4.54 mmol), THF (5 mL), and dimethyl sulfide (5 mL). This reaction mixture was then cooled to -78°C in a dry ice/ethanol bath. Methyl magnesium bromide (3 M, 1.51 mL, 4.54 mmol) was then carefully added to the solution by syringe and the reaction was stirred for 45 min at -78°C . The *N*₃-cinnamoyloxadiazinone (**14**) (0.509 g, 1.51 mmol) was placed into a 25 mL flame-dried glass vial fitted with a rubber septum for nitrogen purging and dissolved in THF (6 mL). This solution was transferred to the addition funnel and added by dropwise addition to the reaction vessel. The reaction stirred for 17 h while it gradually warmed up to room temperature.

The reaction was then diluted with ethyl acetate (80 mL) and washed with 1 M NaOH (20 mL), 1 M HCl (20 mL) and brine solution (20 mL). The recovered organic layer was dried (MgSO₄), filtered under gravity and the solvent removed under high vacuum. The crude product was purified by flash column chromatography (hexanes:ethyl acetate, 70:30) to yield 0.348 g (65%) of the titled compound as a colorless viscous oil. Only the major isomer is reported: ¹H NMR (500 MHz, CDCl₃): δ 0.79 (d, *J* = 7.0 Hz, 3H), 1.32 (d, *J* = 6.8 Hz, 3H), 2.82 (s, 3H), 3.11 (dd, *J* = 7.6, 16.4 Hz, 1H), 3.27–3.49 (m, 3H), 5.99 (d, *J* = 4.4 Hz, 1H), 7.15–7.20 (m, 1H), 7.25–7.29 (m, 6H), 7.31–7.34 (m, 1H), 7.37–7.41 (m, 2H); ¹³C NMR (125 MHz, CDCl₃): δ 12.4, 21.8, 36.2, 43.3, 45.9, 56.8, 124.9, 126.3, 127.1, 128.2, 128.4, 128.7, 135.7, 146.0, 148.4, 172.6; IR (CHCl₃): 1778, 1724, 1257, 1137, 744, 700 cm⁻¹; ESI HRMS for C₂₁H₂₄N₂NaO₃⁺: calcd (M + Na⁺) 375.1679, found 375.1678.

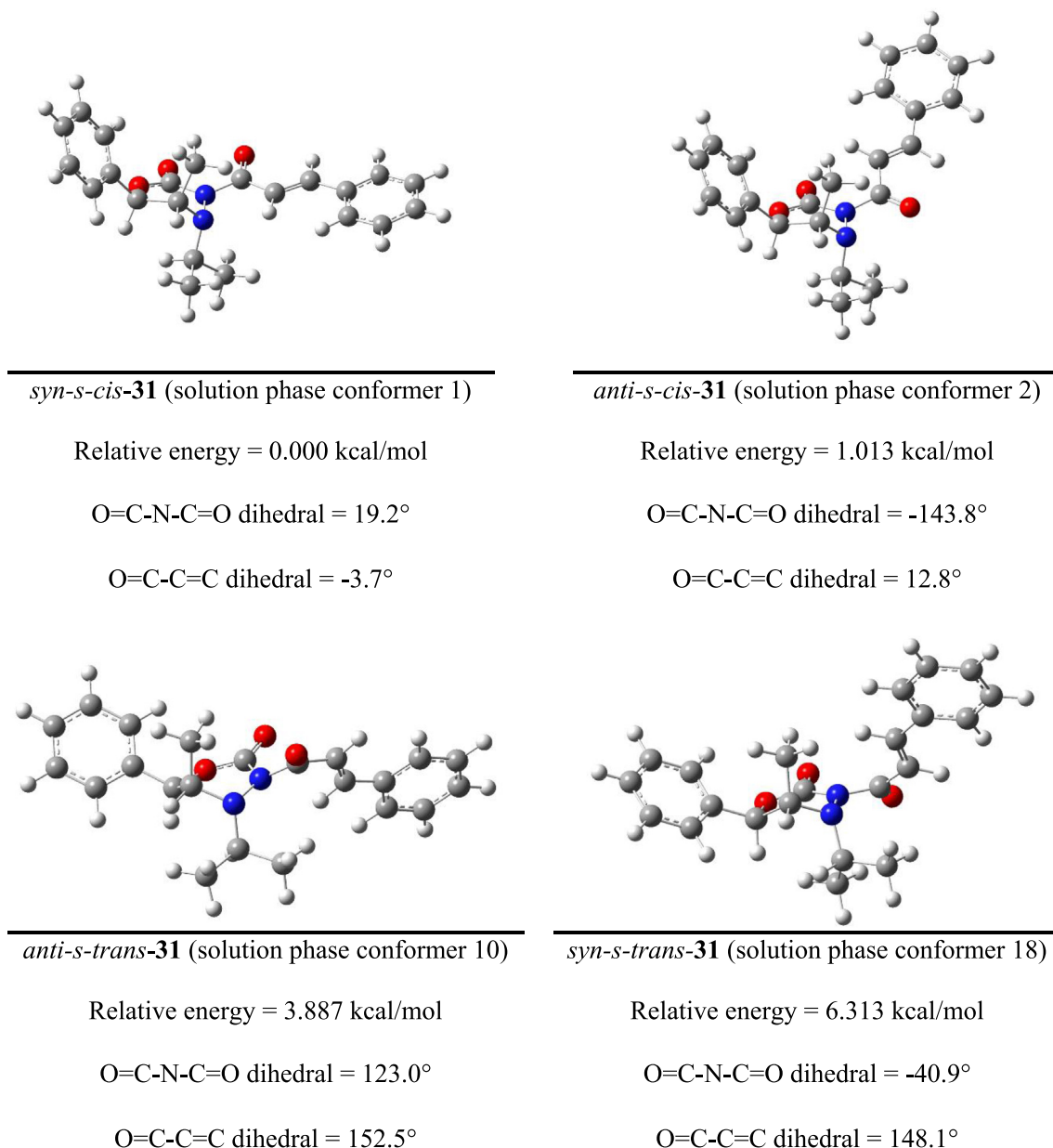


Fig. 8. Lowest energy solution phase conformers of isopropyl-substituted oxadiazinone **31**, ωb97x-D/6-311++G(d,p) level. The O=C-N-C=O dihedral angle corresponds to O25-C2-C15-O24 and the O=C-C=C dihedral angle corresponds to O24-C15-C16-C17.

4.4. Example general procedure for the asymmetric conjugate addition with oxadiazinone **14b**

In a flame dried nitrogen-purged 100 mL, 3-neck round bottom flask fitted with a pressure-equalizing addition funnel chilled to -78 °C was placed CuBr-S(CH₃)₂ (1.65 g, 8.02 mmol), anhydrous THF (16 mL) and dimethyl sulfide (16 mL) and phenylmagnesium bromide (10.6 mmol, 10.6 mL, 1.0 M solution in THF) was added by syringe. The reaction solution was allowed to stir for 5 min before the addition of oxadiazinone **14b** (1.00 g, 3.65 mmol) dissolved in freshly distilled THF (9 mL), delivered via the addition funnel. The reaction stirred for 30 min and determined complete by TLC analysis. The reaction was quenched by the addition of aqueous sodium bicarbonate (75 mL). The resulting mixture was extracted with ethyl acetate (2 × 75 mL) and washed with aqueous sodium

bicarbonate (3 × 75 mL), brine (75 mL), dried (MgSO₄), and the solvents were removed by rotary evaporation. The crude product was then purified by flash chromatography on silica gel.

4.4.1. (5*S*,6*R*)-4,5-dimethyl-3-[3-methylpentanoyl]-6-phenyl-1,3,4-oxadiazinone (**15b**)

The crude product was purified using a mobile phase of 80:20 (hexanes:ethyl acetate) yielding the title compound (0.868, 78%) as a clear yellow oil. The product was obtained as a mixture of diastereomers. The major diastereomer is reported. ¹H NMR (400 MHz, CDCl₃): δ 0.85 (d, *J* = 7.0 Hz, 3H), 0.90 (d, *J* = 7.7 Hz, 3H), 0.96 (d, *J* = 7.7 Hz, 3H), 1.19–1.32 (m, 1H), 1.36–1.46 (m, 1H), 1.97–2.05 (m, 1H), 2.72–3.03 (m, 2H), 2.99 (s, 3H), 3.42 (dq, *J* = 7.0, 4.4 Hz, 1H), 6.04 (d, *J* = 4.4 Hz, 1H), 7.26–7.43 (m, 5H). ¹³C NMR (100 MHz, CDCl₃): δ 11.1, 12.3, 19.0, 29.2, 31.2, 43.2, 44.3, 56.5, 77.6,

Table 3

Results for the first 25 conformers of isopropyl-substituted oxadiazinone **31**, found in the gas phase with the ω b97x-D/6-311++G(d,p) level of theory. The lowest energy conformer of each type is highlighted in gray.

Conformer entry	Classification	Relative E (kcal/mol)	Dipole Moment (Debye)
1	<i>anti-s-cis</i>	0.000	2.647
2	<i>anti-s-cis</i>	0.776	2.806
3	<i>anti-s-cis</i>	1.315	2.278
4	<i>syn-s-cis</i>	1.481	7.575
5	<i>anti-s-cis</i>	2.464	2.733
6	<i>syn-s-cis</i>	2.662	7.054
7	<i>anti-s-cis</i>	2.955	2.475
8	<i>syn-s-cis</i>	2.993	7.700
9	<i>anti-s-cis</i>	3.409	2.952
10	<i>anti-s-cis</i>	3.417	2.779
11	<i>anti-s-trans</i>	3.817	3.413
12	<i>syn-s-cis</i>	3.842	7.655
13	<i>syn-s-cis</i>	4.034	7.140
14	<i>anti-s-trans</i>	4.433	3.345
15	<i>anti-s-cis</i>	4.978	2.410
16	<i>syn-s-cis</i>	5.016	7.026
17	<i>anti-s-cis</i>	5.096	2.425
18	<i>anti-s-trans</i>	5.248	3.958
19	<i>syn-s-cis</i>	5.587	7.152
20	<i>anti-s-cis</i>	6.760	2.814
21	<i>anti-s-cis</i>	6.779	2.272
22	<i>syn-s-cis</i>	7.270	7.161
23	<i>anti-s-cis</i>	7.278	2.288
24	<i>anti-s-cis</i>	7.391	2.320
25	<i>syn-s-trans</i>	7.743	7.802

Table 4

Results for the first 25 conformers of isopropyl-substituted oxadiazinone **31** found in solution phase (chloroform) at the ω b97x-D/6-311++G(d,p) level of theory. The lowest energy conformer of each type is highlighted in gray.

Conformer entry	Classification	Relative E (kcal/mol)
1	<i>syn-s-cis</i>	0.000
2	<i>anti-s-cis</i>	1.013
3	<i>anti-s-cis</i>	1.722
4	<i>syn-s-cis</i>	1.768
5	<i>anti-s-cis</i>	2.017
6	<i>syn-s-cis</i>	2.097
7	<i>anti-s-cis</i>	3.472
8	<i>syn-s-cis</i>	3.527
9	<i>anti-s-cis</i>	3.764
10	<i>anti-s-trans</i>	3.887
11	<i>syn-s-cis</i>	4.003
12	<i>anti-s-cis</i>	4.010
13	<i>syn-s-cis</i>	4.181
14	<i>anti-s-cis</i>	4.371
15	<i>anti-s-trans</i>	4.399
16	<i>anti-s-trans</i>	4.937
17	<i>anti-s-cis</i>	6.128
18	<i>syn-s-trans</i>	6.313
19	<i>anti-s-cis</i>	6.319
20	<i>syn-s-trans</i>	6.321
21	<i>syn-s-trans</i>	6.605
22	<i>syn-s-cis</i>	6.930
23	<i>anti-s-cis</i>	7.071
24	<i>anti-s-cis</i>	8.574
25	<i>anti-s-cis</i>	8.678

124.7, 128.0, 128.5, 135.5, 148.2, 173.2. IR (neat): 1720, 746, 700 cm^{-1} . EI-HRMS: calcd for $\text{C}_{17}\text{H}_{24}\text{N}_2\text{O}_3$: 304.1785. Found: 304.1787.

4.4.2. (5*S*,6*R*)-4,5-dimethyl-6-phenyl-3-[3-phenylbutanoyl]-1,3,4-oxadiazinone (**15c**)

The crude product was purified using a mobile phase of 65:35 (hexanes:ethyl acetate) yielding the title compound (0.897, 70%) as

a clear yellow oil. The product was obtained as a mixture of diastereomers. The major diastereomer is reported. ^1H NMR (400 MHz, CDCl_3): δ 0.56 (d, $J = 7.0$ Hz, 3H), 1.34 (d, $J = 7.0$ Hz, 3H), 3.00 (s, 3H), 3.06–3.18 (m, 1H), 3.27–3.47 (m, 3H), 5.99 (d, $J = 4.4$ Hz, 1H), 7.12–7.42 (m, 10H). ^{13}C NMR (100 MHz, CDCl_3): δ 11.9, 21.8, 36.1, 43.0, 45.5, 56.3, 77.6, 124.6, 126.0, 126.8, 127.9, 128.2, 128.4, 135.4, 145.5, 148.1, 172.3. IR (CDCl_3): 1777, 1731, 746, 700 cm^{-1} . EI-HRMS: calcd for $\text{C}_{21}\text{H}_{24}\text{N}_2\text{O}_3$: 352.1786. Found: 352.1787.

4.4.3. (5*S*,6*R*)-4,5-dimethyl-6-phenyl-3-[3-(*p*-methoxybutanoyl)-1,3,4-oxadiazinone (**15d**)

The crude product was purified using a mobile phase of 60:40 (hexanes:ethyl acetate) yielding the title compound (0.997 g, 67%) as a clear yellow oil. The product was obtained as a mixture of diastereomers. The major diastereomer is reported. ^1H NMR (400 MHz, CDCl_3): δ 0.58 (d, $J = 7.0$ Hz, 3H), 1.31 (d, $J = 7.0$ Hz, 3H), 2.88 (s, 3H), 3.05–3.13 (m, 1H), 3.29–3.42 (m, 2H), 3.72 (s, 3H), 5.99 (d, $J = 4.4$ Hz, 1H), 6.82 (m, 2H), 7.17–7.39 (m, 9H). ^{13}C NMR (100 MHz, CDCl_3): δ 11.6, 21.6, 34.9, 42.6, 45.2, 54.5, 55.9, 83.1, 113.2, 124.3, 127.3, 127.5, 128.0, 135.2, 137.4, 147.6, 157.4, 172.0. IR (neat): 1776, 1723, 765, 700 cm^{-1} . EI-HRMS (calcd for $\text{C}_{22}\text{H}_{26}\text{N}_2\text{O}_4$: 382.1886. Found: 382.1892.

4.5. (4*S*,5*S*)-3-*trans*-cinnamoyl-4,5-dimethyl-6-phenyl-1,3,4-oxadiazinone (**19**)

trans-Cinnamic acid (2.58 g, 17.4 mmol) was added to a flame dried, nitrogen purged 250 mL round bottom flask and dissolved in anhydrous dichloromethane (16 mL). This was followed with a sequential addition of 1-ethyl-3-(3-dimethylaminopropyl)carbodiimide (EDC, 3.34 g, 17.4 mmol), DMAP (0.268 g, 2.18 mmol) and oxadiazinone **9b** (1.80 g, 8.72 mmol). The reaction was stirred for 16 h at room temperature after which the reaction was diluted with dichloromethane (80 mL) and sequentially treated with 1 M HCl (20 mL), 1 M NaOH (2 \times 20 mL), and brine (20 mL). The organic layer was dried (MgSO_4), gravity filtered, and the solvent was removed under reduced pressure. The crude product obtained was purified by flash column chromatography (hexanes: ethyl acetate, 75:25) to yield the title compound (1.74 g, 59%) as a white fluffy solid. *mp*: 47–50 $^\circ\text{C}$. ^1H NMR (500 MHz, CDCl_3): δ 1.21 (d, $J = 6.8$ Hz, 3H), 2.91 (s, 3H), 3.42 (dq, $J = 6.8, 10.4$ Hz, 1H), 5.30 (d, $J = 9.8$ Hz, 1H), 7.36–7.38 (m, 2H), 7.42–7.45 (m, 6H), 7.53 (d, $J = 15.7$ Hz, 1H), 7.62–7.64 (m, 1H), 7.89 (d, $J = 15.7$ Hz, 1H); ^{13}C NMR (125 MHz, CDCl_3): δ 15.4, 38.7, 61.0, 84.1, 118.7, 126.9, 128.4, 128.9, 129.0, 129.3, 130.5, 134.8, 136.0, 145.8, 149.5, 165.8; IR (CHCl_3): 1704, 1626, 1577, 1204, 1128, 1045, 700 cm^{-1} . ESI HRMS for $\text{C}_{20}\text{H}_{20}\text{N}_2\text{NaO}_3$: calcd (M + Na $^+$) 359.1366, found 359.1358.

4.6. (5*S*,6*S*)-4,5-dimethyl-6-phenyl-3-(3'-phenylbutanoyl)-1,3,4-oxadiazinone (**20**)

To a 100 mL flame-dried, nitrogen-purged three-neck round bottomed flask fitted centrally with a 60 mL addition funnel was added copper bromide dimethyl sulfide complex (1.00 g, 4.87 mmol), tetrahydrofuran (5 mL), and dimethyl sulfide (5 mL). This reaction mixture was then cooled to -78 $^\circ\text{C}$ in a dry ice/ethanol bath. Methyl magnesium bromide (3 M, 1.62 mL, 4.86 mmol) was then carefully added to the solution by syringe and the reaction was stirred for 45 min at -78 $^\circ\text{C}$. The N_3 -cinnamoyloxadiazinone (**19**) (0.546 g, 1.62 mmol) was placed into a 25 mL flame-dried glass vial fitted with a rubber septum for nitrogen purging and dissolved in THF (6 mL). This solution was transferred to the addition funnel and added by dropwise addition to the reaction vessel. The reaction stirred for 17 h while it gradually

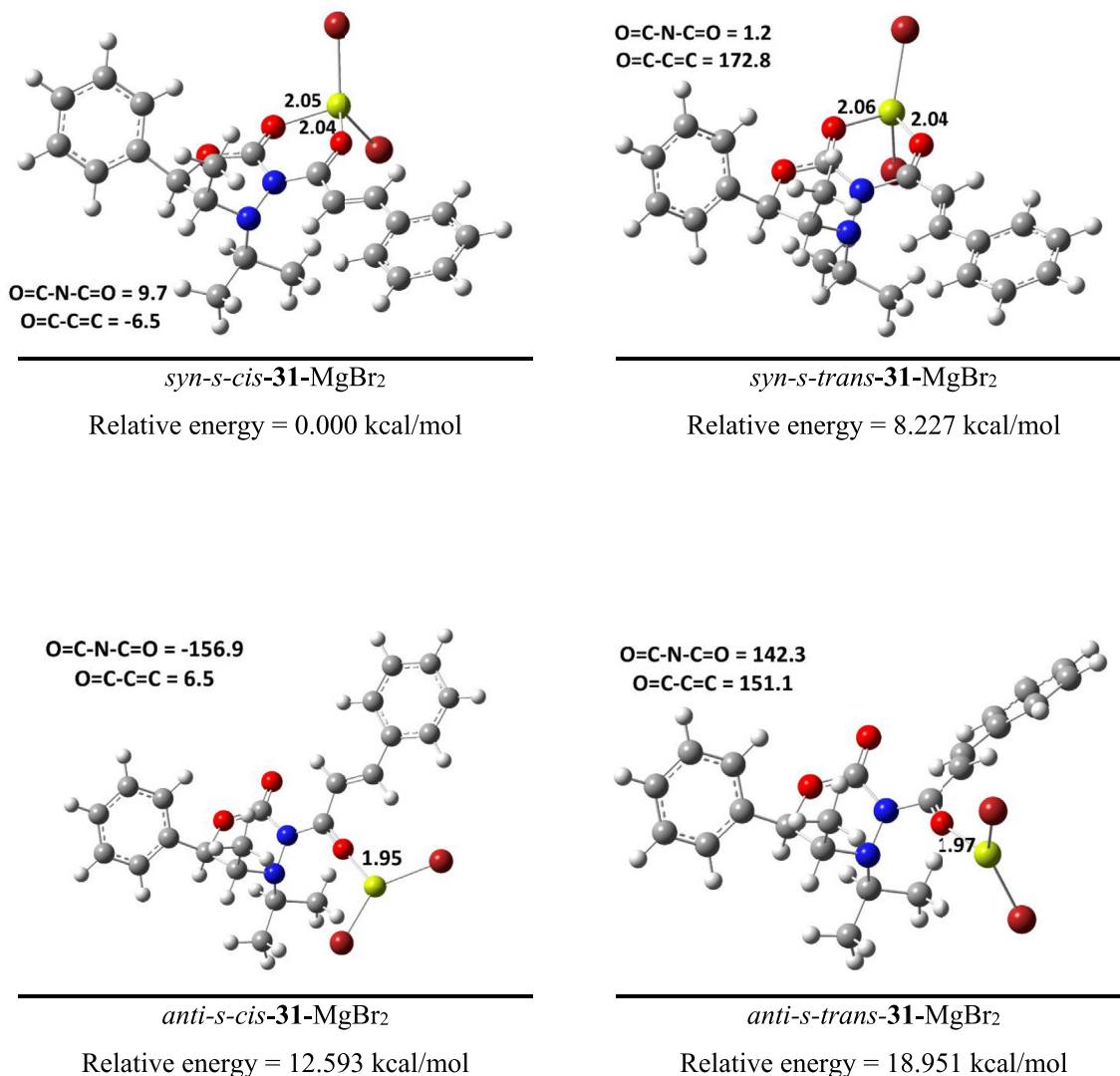


Fig. 9. Optimized structures for MgBr_2 interacting with each conformation of oxadiazinone **31** in chloroform at the B3LYP/6-31G(d) level. The $\text{O}=\text{C}-\text{N}-\text{C}=\text{O}$ dihedral angle shown corresponds to O25–C2–C15–O24 and the $\text{O}=\text{C}-\text{C}=\text{C}$ dihedral angle corresponds to O24–C15–C16–C17.

warmed up to room temperature. The reaction was then diluted with ethyl acetate (80 mL) and washed with 1 M NaOH (20 mL), 1 M HCl (20 mL) and brine solution (20 mL). The recovered organic layer was dried (MgSO_4), filtered under gravity and solvent was removed under high vacuum. The crude product was purified by flash column chromatography (hexanes:ethyl acetate, 70:30) to yield 0.451 g (79%) of the titled compound as a colorless oil that was determined to be a mixture of diastereomers in which there was observable line broadening. ^1H NMR (500 MHz, CDCl_3): δ 0.96 (d, $J = 6.8$ Hz, 3H), 1.29 (d, $J = 6.9$ Hz, 3H), 2.62 (s, 3H), 2.90–3.04 (m, 2H), 3.25–3.29 (dd, $J = 7.7, 15.7$ Hz, 1H), 3.35 (sextet, $J = 7.1$ Hz, 1H), 5.1 (bs, 1H), 7.13–7.18 (m, 4H), 7.21–7.24 (m, 3H), 7.31–7.33 (m, 3H); ^{13}C NMR (125 MHz, CDCl_3): δ 15.6, 22.0, 36.8, 36.9, 44.7, 45.1, 83.9, 126.5, 126.9, 127.1, 128.5, 128.6, 128.9, 129.3, 135.9, 145.9, 171.9; IR (neat): 1781, 1728, 1211, 1126, 760, 700 cm^{-1} . ESI HRMS for $\text{C}_{21}\text{H}_{24}\text{N}_2\text{NaO}_3^+$: calcd (M + Na^+) 375.1679, found 375.1673.

4.7. N3-trans-cinnamoyl-N4-p-methoxybenzyl-5-methyl-6-phenyl-1,3,4-oxadiazinone (25)

trans-Cinnamic acid (0.807 g, 5.45 mmol) was added to a flame-

dried, nitrogen-purged 250 mL round bottom flask and dissolved in anhydrous dichloromethane (16 mL). This was followed with the addition of 1-ethyl-3-(3-dimethylaminopropyl)carbodiimide (EDC) (1.05 g, 5.45 mmol), DMAP (0.110 g, 0.900 mmol) and the oxadiazinone **22** (1.42 g, 4.54 mmol). The reaction was then stirred for 16 h at room temperature after which the reaction was diluted with dichloromethane (80 mL) and washed with 1 M HCl (20 mL), 1 M NaOH (2×20 mL) followed by brine (20 mL) wash. The organic layer was dried (MgSO_4), gravity filtered, and solvent was removed under reduced pressure. The crude product obtained was purified by flash column chromatography (hexanes:ethyl acetate, 80:20) to yield 1.14 g (80%) of the title compound as a white fluffy solid: *mp*: 57–61 $^\circ\text{C}$. ^1H NMR (500 MHz, CDCl_3): δ 0.85 (d, $J = 7.0$ Hz, 3H) 3.47 (dq, $J = 4.8, 7.0$ Hz, 1H) 3.82 (s, 3H) 4.20 (d, $J = 12.5$ Hz, 1H) 4.39 (d, $J = 12.5$ Hz, 1H) 6.14 (d, $J = 4.6$ Hz, 1H) 6.94 (d, $J = 8.6$ Hz, 2H) 7.26 (d, $J = 7.8$ Hz, 2H) 7.33 (t, $J = 7.3$, 1H), 7.39 (d, $J = 7.8$, 2H) 7.41–7.43 (m, 3H), 7.47 (d, $J = 8.6$ Hz, 2H) 7.52 (d, $J = 15.7$ Hz, 1H) 7.59 (m, 2H) 7.78 (d, $J = 15.7$ Hz, 1H). ^{13}C NMR (125 MHz, CDCl_3): δ 12.5, 52.0, 55.3, 59.3, 78.0, 114.4, 119.1, 124.9, 127.0, 128.2, 128.4, 128.7, 128.8, 130.4, 130.7, 134.9, 135.9, 145.4, 148.2, 159.8, 166.8. IR (CHCl_3): 1760, 1727, 1615, 1247, 1216, 1136, 823, 736, 701 cm^{-1} . ESI-HRMS calc'd for

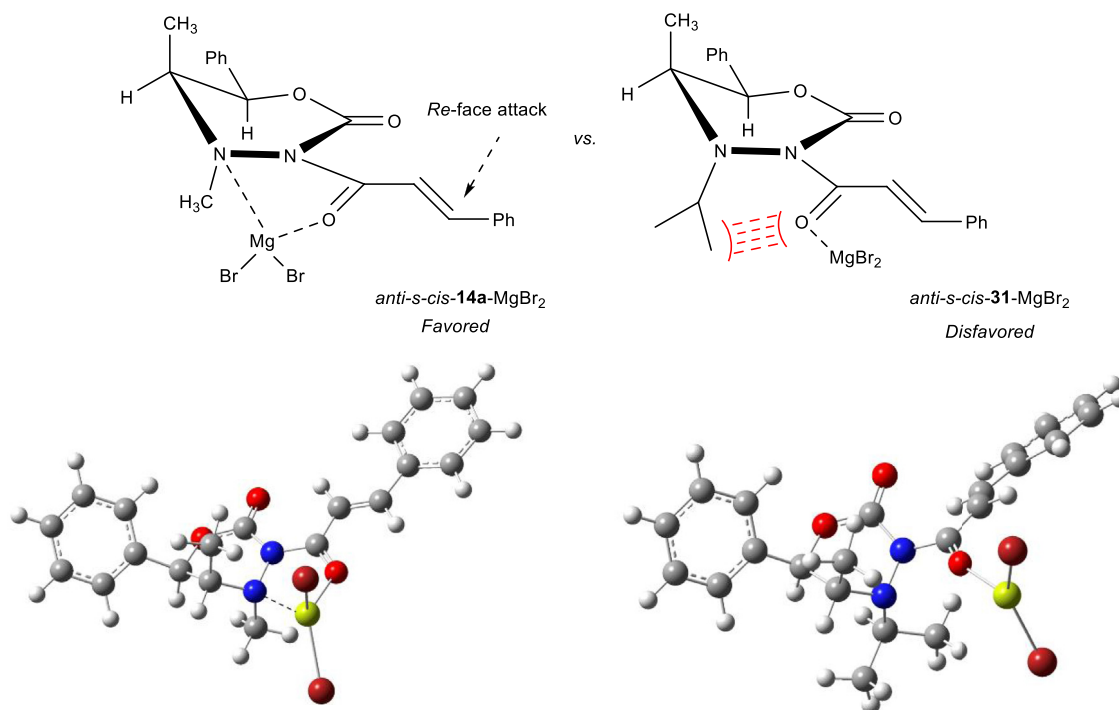


Fig. 10. Comparison of key intermediates in the conjugate addition pathways with oxadiazinones **14a** and **31**.

$C_{27}H_{26}N_2NaO_4$ ($M + Na^+$): 465.1785. Found: 465.1779.

4.8. *N*₃-*trans*-crotonyl-*N*₄-*p*-methoxybenzyl-5-methyl-6-phenyl-1,3,4-oxadiazinone (**26**)

To a flame-dried, nitrogen-purged 100 mL round bottom flask was added the oxadiazinone **22** (0.50 g, 1.6 mmol) which was dissolved in DMF (8.00 mL). To the solution was added sodium hydride (0.077 g, 3.2 mmol). The reaction was stirred for 10 min and crotonyl chloride (0.17 mL, 1.8 mmol) was then added. The reaction stirred for an additional 18 h at room temperature, after which it was diluted with dichloromethane (50 mL) and washed with 1 M HCl (20 mL) and brine (20 mL). The organic layer was dried ($MgSO_4$), gravity filtered, and the solvent removed under reduced pressure. The title compound was isolated as a yellow solid in a yield of 0.595 g (98%) after purification by flash column chromatography (hexanes: ethyl acetate, 80:20): $mp = 54-56^\circ C$. 1H NMR (500 MHz, $CDCl_3$): δ 0.77 (d, $J = 6.9$ Hz, 3H), 1.93 (dd, $J = 1.4, 6.9$, 3H), 3.38 (dq, $J = 4.5, 7.0$ Hz, 1H) 3.83 (s, 3H) 4.13 (d, $J = 12.6$ Hz, 1H) 4.31 (d, $J = 12.6$ Hz, 1H) 6.07 (d, $J = 4.5$ Hz, 1H) 6.92 (d, $J = 8.5$ Hz, 2H) 7.07 (dq, $J = 7.5, 15.2$ Hz, 1H) 7.20 (d, $J = 7.5, 2H$) 7.26–7.37 (m, 4H), 7.42 (d, $J = 8.5$ Hz, 2H); ^{13}C NMR (125 MHz, $CDCl_3$): δ 12.4, 18.5, 51.5, 55.3, 59.1, 77.9, 114.3, 123.6, 124.9, 127.0, 128.1, 128.7, 130.7, 135.9, 145.7, 148.2, 159.7, 166.6; IR ($CHCl_3$): 1762, 1725, 1639, 1248, 790, 823, 733 cm^{-1} . ESI-HRMS calc'd for $C_{22}H_{24}N_2NaO_4$ ($M + Na^+$): 403.1628. Found: 403.1622.

4.9. *N*₄-*p*-methoxybenzyl-5-methyl-6-phenyl-3-(3'-phenylbutanoyl)-1,3,4-oxadiazinone (**27**) derived from oxadiazinone **25**

To a flame dried, nitrogen-purged, three-neck 100 mL round bottomed flask centrally fitted with a 60 mL addition funnel was added copper bromide-dimethyl sulfide complex (0.696 g, 3.39 mmol), THF (5 mL), and dimethyl sulfide (5 mL). The reaction

was then cooled to $-78^\circ C$ and methyl magnesium bromide (3 M, 1.13 mL, 3.39 mmol) was then carefully added to the solution by syringe and the solution stirred for 45 min at $-78^\circ C$. The *N*₃-cinnamoyloxadiazinone (**25**) substrate (0.500 g, 1.13 mmol) was placed into a 25 mL flame-dried glass vial fitted with a rubber septum for nitrogen purging and dissolved in THF (6 mL). This solution was transferred to the addition funnel and added by dropwise addition to the reaction vessel. The reaction stirred for 17 h while it gradually warmed up to room temperature. The reaction was then diluted with ethyl acetate (80 mL) and washed with 1 M NaOH (20 mL), 1 M HCl (20 mL) and brine solution (20 mL). The recovered organic layer was dried ($MgSO_4$), filtered under gravity and solvent was removed under high vacuum. The crude product was purified by flash column chromatography (hexanes: ethyl acetate, 80:20) to yield 0.321 g (60%) of the titled compound as a yellow viscous oil as a mixture of diastereomers. Only the major diastereomer is reported. 1H NMR (500 MHz, $CDCl_3$): δ 0.61 (d, $J = 7.0$ Hz, 3H), 1.20 (d, $J = 6.9$ Hz, 3H), 2.95 (dd, $J = 7.9, 16.7$ Hz, 1H), 3.22–3.27 (m, 3H), 3.30–3.37 (m, 1H), 3.75 (s, 3H), 3.92 (d, $J = 12.5, 1H$), 4.01 (d, $J = 12.5, 1H$), 5.93 (d, $J = 4.5, 1H$), 6.82–6.85 (m, 2H), 7.07–7.11 (m, 3H), 7.17–7.20 (m, 5H), 7.25–7.28 (m, 2H), 7.32–7.34 (m, 2H). ^{13}C NMR (125 MHz, $CDCl_3$): δ 12.3, 21.9, 36.0, 45.6, 51.4, 55.3, 58.7, 77.9, 114.3, 124.8, 126.2, 127.0, 127.1, 128.1, 128.5, 128.7, 130.7, 135.9, 146.2, 148.4, 159.8, 172.6. ESI-HRMS calc'd for $C_{28}H_{30}N_2NaO_4$ ($M + Na^+$): 481.2098. Found: 481.2099.

4.10. *N*₄-*p*-methoxybenzyl-5-methyl-6-phenyl-3-(3'-phenylbutanoyl)-1,3,4-oxadiazinone (**27**) derived from oxadiazinone **26**

To a flame dried, nitrogen-purged, three-neck 100 mL round bottomed flask centrally fitted with a 60 mL separatory funnel was added copper bromide dimethyl sulfide complex (0.580 g, 2.82 mmol), THF (5 mL) and dimethyl sulfide (5 mL). The reaction was then cooled to $-78^\circ C$ and methyl magnesium bromide (3 M,

0.940 mL, 2.82 mmol) was then carefully added to the solution and the reaction stirred for 45 min at -78°C . The N_3 -crotonyloxadiaxinone (**26**) was placed into a 25 mL flame-dried glass vial fitted with a rubber septum for nitrogen purging and dissolved in THF (6 mL). This solution was transferred to the addition funnel and added by dropwise addition to the reaction vessel. The reaction stirred for 17 h while it gradually warmed up to room temperature. The reaction was then diluted with ethyl acetate (80 mL) and washed with 1 M NaOH (20 mL), 1 M HCl (20 mL) and brine solution (20 mL). The recovered organic layer was dried with magnesium sulfate, filtered under gravity and solvent removed under high vacuum. The crude product obtained was purified by flash column chromatography (hexanes: ethyl acetate, 70:30) to yield 0.224g (52%) of the titled compound as a yellow viscous oil as a mixture of diastereomers. Only the major diastereomer is reported: ^1H NMR (500 MHz, CHCl_3): δ 0.58 (d, $J = 7.0$ Hz, 3H), 1.33 (d, $J = 7.0$ Hz, 3H), 3.17 (dd, $J = 7.3, 16.7$ Hz, 1H), 3.29–3.33 (m, 2H), 3.35–3.38 (sxt, $J = 6.9$ Hz, 1H), 3.85 (s, 3H), 4.07 (d, $J = 12.4$, 1H), 4.19 (d, $J = 12.4$, 1H), 6.05 (d, $J = 4.6$, 1H), 6.93–6.96 (m, 2H), 7.17–7.21 (m, 3H), 7.26–7.32 (m, 4H), 7.35–7.38 (m, 2H), 7.42–7.47 (m, 3H); ^{13}C NMR (125 MHz, CHCl_3): δ 12.2, 22.1, 36.2, 45.6, 51.2, 55.3, 58.6, 78.0, 114.3, 124.8, 126.3, 127.0, 128.1, 128.5, 128.7, 128.8, 130.6, 135.9, 146.1, 148.7, 159.7, 172.5; IR (CHCl_3): 1775, 1726, 1213, 1136, 850, 740, 700 cm^{-1} . ESI-HRMS calc'd for $\text{C}_{28}\text{H}_{30}\text{N}_2\text{NaO}_4$ ($\text{M} + \text{Na}^+$): 481.2098. Found: 481.2100.

4.11. (*S*)-(+)-3-phenylbutanoic acid (**16**) derived from the oxidative cleavage of the diastereomeric mixture of oxadiazinone **27**

Into a 250 mL round bottomed flask was added oxadiazinone **27** (1.26 g, 2.74 mmol) and acetonitrile (50 mL). To the homogenized mixture was added ceric ammonium nitrate (7.53 g, 13.7 mmol) pre-dissolved in deionized water (50 mL). The reaction was stirred for 3 h. The reaction solvent was thereafter removed under reduced pressure. The concentrated solution was then reconstituted with diethyl ether (50 mL) and treated with brine solution (30 mL) to effect the removal of residual cerium ammonium nitrate. The organic layer was then treated with 1 M NaOH (30 mL). The aqueous layer was collected and treated with 3 M HCl (30 mL) and extracted with diethyl ether (50 mL). The collected organic layer was treated with brine, dried (MgSO_4), and the solvent was removed under reduced pressure. This material and was purified by flash column chromatography (hexanes:ethyl acetate, 80:20). This process yielded the title compound (0.10 g, 22%) as a colorless oil: $[\alpha]_D^{25} = +22$. ^1H NMR (500 MHz, CHCl_3): δ 1.33 (d, $J = 7.0$ Hz, 3H), 2.58 (dd, $J = 15.5, 8.2$, Hz, 1H), 2.68 (dd, $J = 6.8$ Hz, 1H), 3.28 (sxt, $J = 7.0$ Hz, 1H), 7.19–0.23 (m, 3H), 7.29–7.32 (m, 2H). ^{13}C NMR (CHCl_3): δ 21.9, 36.2, 42.6, 126.5, 126.7, 128.6, 145.5, 178.5; IR (neat): 2970, 1706, 1296, 763, 700 cm^{-1} . ESI-HRMS for $\text{C}_{11}\text{H}_{14}\text{N}_2\text{NaO}_2^+$: calc'd ($\text{M} + \text{Na}^+$) 187.0730, found 187.0730.

4.12. *N*3-*trans*-cinnamoyl-*N*4-isopropyl-5-methyl-6-phenyl-1,3,4-oxadiazinone (**31**)

In a flame-dried, nitrogen purged 1 L round bottomed flask fitted with a condenser was placed oxadiazinone **30** (5.00 g, 21.3 mmol), dissolved in methylal chloride (25 mL). To this stirred mixture was added *trans*-cinnamoyl chloride (4.25 g, 25.5 mol). This mixture was heated to reflux and then lithium hydride (0.18 g, 22.4 mmol) was added. The reaction stirred for 18 h and was then cooled to room temperature and quenched with a saturated solution of sodium bicarbonate (50 mL). The target product was extracted with methylene chloride (3×20 mL), and the extract was washed with brine (30 mL), dried (MgSO_4). The solvents were removed under reduced pressure and the crude product was

purified by flash chromatography (hexanes:ethyl acetate, 85:15). The isolated product was recovered as a yellow oil (7.52 g, 95%). ^1H NMR (400 MHz, CDCl_3): δ 0.83 (d, $J = 6.6$ Hz, 3H), 1.19 (d, $J = 6.6$ Hz, 3H), 1.37 (d, $J = 6.3$ Hz, 3H), 3.47 (septet, $J = 6.3$ Hz, 1H), 3.81 (m, 1H), 5.97 (d, $J = 5.1$ Hz, 1H), 7.24–7.37 (m, 10H). ^{13}C NMR (100 MHz, CDCl_3): δ 13.4, 20.9, 21.2, 52.0, 54.6, 79.1, 118.7, 125.1, 128.4, 128.6, 129.1, 130.7, 135.0, 136.2, 146.1, 148.4, 168.0; IR (neat): 3031, 1759, 1725, 1619, 1218, 1024, 742, 700 cm^{-1} . EI-HRMS calc'd for $\text{C}_{22}\text{H}_{24}\text{N}_2\text{NaO}_3$ (M^+): 364.1787. Found: 364.1787.

4.13. *N*4-isopropyl-5-methyl-6-phenyl-3-(3'-phenylbutanoyl)-1,3,4-oxadiazinone (**32**)

In a flame-dried, nitrogen-purged three-necked 100 ml round bottom flask equipped with a pressure-equalizing addition funnel was placed copper(I) bromide-dimethyl sulfide complex (1.02 g, 4.97 mmol), dimethyl sulfide (5 mL), and THF (10 mL). The reaction vessel was then cooled to -78°C and methylmagnesium bromide (1 M, 8.3 mL, 8.3 mmol) was added to the reaction vessel via syringe. The reaction mixture in the round bottom flask stirred for an additional 20 min. To the addition funnel was added the oxadiazinone **31** (0.25 g, 0.83 mmol) dissolved in THF (5 mL). The oxadiazinone was added by dropwise addition to the reaction mixture, and after the addition the reaction mixture stirred for an additional 2 h. The reaction was quenched by the addition of a saturated aqueous sodium bicarbonate. The desired product was then extracted with ethyl acetate (2×20 mL) and the organic solution was washed with a saturated solution of brine (20 mL). The organic layer was then dried (MgSO_4), and the solvents were removed under reduced pressure. This process afforded a yellow oil that was purified by flash chromatograph (hexanes:ethyl acetate, 80:20) to yield the target compound as a viscous oil (0.142 g, 0.455 mol) in 55% yield. ^1H NMR (400 MHz, CDCl_3): δ 0.41 (d, $J = 6.6$ Hz, 3H), 0.72 (d, $J = 6.6$ Hz, 3H), 0.94 (d, $J = 6.3$ Hz, 3H), 1.11 (d, $J = 6.3$ Hz, 3H), 1.29–1.34 (m, 2H), 3.07–3.14 (m, 1H), 3.33 (septet, $J = 6.3$ Hz, 1H), 3.75 (dq, $J = 13.7, 6.6$ Hz, 1H), 5.92 (d, 5.1 Hz, 1H), 7.16–7.40 (m, 10H). ^{13}C NMR (100 MHz, CDCl_3): δ 13.2, 20.6, 20.8, 21.9, 36.0, 46.0, 51.6, 79.1, 115.6, 125.0, 126.5, 127.4, 128.4, 128.6, 128.9, 136.2, 146.3, 173.6; IR (neat): 1726, 1605, 1243, 1168, 1022, 754, 700 cm^{-1} . ESI-HRMS calc'd for $\text{C}_{23}\text{H}_{29}\text{N}_2\text{NaO}_3$ ($\text{M} + \text{Na}^+$): 381.2178. Found: 381.2178.

Declaration of competing interest

The authors declare that they have no known competing financial interests or personal relationships that could have appeared to influence the work reported in this paper.

Acknowledgements

We thank the Department of Chemistry of Illinois State University for an internal summer research grant for Fatima Olayemi Obe. Acknowledgment is made to the National Science Foundation (NSF) for SC-XRD (CHE-1039689) analyses from Departmental instrumentation obtained from the Major Research Instrumentation (MRI) program.

Appendix A. Supplementary data

Supplementary data to this article can be found online at <https://doi.org/10.1016/j.tet.2021.132002>.

References

- [1] K.M. Byrd, Beilstein J. Org. Chem. 11 (2015) 530–562.

- [2] D. Vargova, I. Nemethova, K. Plevova, R. Sebesta, *ACS Catal.* 9 (2019) 3104–3143.
- [3] P. Ramesh, D. Suman, K.S.N. Reddy, *Synthesis* 50 (2018) 211–226.
- [4] A. Mondal, S. Bhowmick, A. Ghosh, T. Chanda, K.C. Bhowmick, *Tetrahedron Asymmetry* 28 (2017) 849–875.
- [5] (a) S.G. Davies, A.M. Fletcher, P.M. Roberts, J.E. Thomson, *Org. Biomol. Chem.* 17 (2019) 1322–1335.
- [6] (a) V. Zadsirjan, M.M. Heravi, *Curr. Org. Synth.* 15 (2018) 3–20.
- [7] M. Heravi, V. Zadsirjan, *Tetrahedron Asymmetry* 24 (2013) 1149–1188.
- [8] W. Zhi, J. Li, D. Zou, Y. Wu, Y. Wu, *J. Org. Chem.* 82 (2017) 12286–12293.
- [9] Z. Leitis, V. Lūsis, *Tetrahedron Asymmetry* 27 (2016) 843–851.
- [10] S. Yodwaree, D. Soorukram, C. Kuharkam, P. Tuchinda, V. Reutrakul, M. Pohmakotr, *Org. Biomol. Chem.* 12 (2014) 6885–6894.
- [11] R. Sabala, L. Hernández-García, A. Ortiz, M. Romero, H.F. Olivo, *Org. Lett.* 12 (2010), 4368 4270.
- [12] J.E. Hein, J. Zimmerman, M.P. Sibi, P.G. Hultin, *Org. Lett.* 7 (2005) 2755–2758.
- [13] (a) J. Dambacher, M. Bergdahl, *J. Org. Chem.* 70 (2005) 580–589; (b) J. Dambacher, R. Anness, P. Pollock, M. Bergdahl, *Tetrahedron* 60 (2004) 2097–2110.
- [14] M.P. Sibi, J. Ji, J.B. Sausker, C.P. Jaspere, *J. Am. Chem. Soc.* 121 (1999) 7517–7526.
- [15] P.G. Andersson, H.E. Schink, K. Osterlund, *J. Org. Chem.* 63 (1998) 8067–8070.
- [16] C.L. Schrank, M.W. Danneman, E.A. Prebihalo, R.E. Anderson, T.J. Gibson, W.M. Wuest, R.J. Mullins, *Tetrahedron Lett.* 61 (2020) 151945.
- [17] (a) R. Sabala, S. Assad, A. Mendoza, J. Jiménez, E. Sansinenea, A. Ortiz, *Tetrahedron Lett.* 60 (2019) 1741–1744; (b) S. Assad, R. Sabala, J. Jiménez, E. Sansinenea, A. Ortiz, *Tetrahedron Lett.* 60 (2019) 1646–1648.
- [18] H. Kaneko, S. Takahashi, N. Kogure, M. Kitajima, H. Takayama, *J. Org. Chem.* 84 (2019) 5645–5654.
- [19] A. Leise, N. Comas, D. Harrison, D. Patel, E. Whitemiller, J. Wilson, J. Timms, I. Golightly, C.G. Hamaker, S.R. Hitchcock, *Tetrahedron Asymmetry* 28 (2017) 1154–1162.
- [20] M.D. Squire, R.A. Davis, K.A. Chianakas, G.M. Ferrence, J.M. Standard, S.R. Hitchcock, *Tetrahedron: Asymmetry* 16 (2005) 1047–1053.
- [21] J.R. Burgeson, D.D. Dore, J.M. Standard, S.R. Hitchcock, *Tetrahedron* 61 (2005) 10965–10974.
- [22] J.F. Vaughn, S.R. Hitchcock, *Tetrahedron: Asymmetry* 15 (2004) 3449–3455.
- [23] S.R. Hitchcock, D.M. Casper, J.F. Vaughn, J.M. Finefield, G.M. Ferrence, J.M. Esken, *J. Org. Chem.* 69 (2004) 714–718.
- [24] (a) D.M. Casper, J.R. Burgeson, J.M. Esken, G.M. Ferrence, S.R. Hitchcock, *Org. Lett.* 4 (2002) 3739–3742; (b) S.R. Hitchcock, G.P. Nora, D.M. Casper, M.D. Squire, C.D. Maroules, G.M. Ferrence, L.F. Szczepura, J.M. Standard, *Tetrahedron* 57 (2001) 9789–9798.
- [25] A.T. Messmer, S. Steinwand, K.M. Lippert, P.R. Schreiner, J. Bredenbeck, *J. Org. Chem.* 77 (2012) 11091–11095.
- [26] T.A. Halgren, *J. Comput. Chem.* 117 (1996) 490–519.
- [27] R. Dennington, T. Keith, J. Millam, *GMMX and GaussView Version 6.1.1*, Semichem Inc., Shawnee Mission KS, 2019.
- [28] M.J. Frisch, G.W. Trucks, H.B. Schlegel, G.E. Scuseria, M.A. Robb, J.R. Cheeseman, G. Scalmani, V. Barone, G.A. Petersson, H. Nakatsuji, X. Li, M. Caricato, A. Marenich, J. Bloino, B.G. Janesko, R. Gomperts, B. Mennucci, H.P. Hratchian, J.V. Ortiz, A.F. Izmaylov, J.L. Sonnenberg, D. Williams-Young, F. Ding, F. Lipparini, F. Egidi, J. Goings, B. Peng, A. Petrone, T. Henderson, D. Ranasinghe, V.G. Zakrzewski, J. Gao, N. Rega, G. Zheng, W. Liang, M. Hada, M. Ehara, K. Toyota, R. Fukuda, J. Hasegawa, M. Ishida, T. Nakajima, Y. Honda, O. Kitao, H. Nakai, T. Vreven, K. Throssell, Montgomery Jr., J.E. Peralta, F. Ogliaro, M. Bearpark, J.J. Heyd, E. Brothers, K.N. Kudin, V.N. Staroverov, T. Keith, R. Kobayashi, J. Normand, K. Raghavachari, A. Rendell, J.C. Burant, S.S. Iyengar, J. Tomasi, M. Cossi, J.M. Millam, M. Klene, C. Adamo, R. Cammi, J.W. Ochterski, R.L. Martin, K. Morokuma, O. Farkas, J.B. Foresman, D.J. Fox, *Gaussian 09*, Revision D.01, Gaussian, Inc., Wallingford CT, 2016.
- [29] E.D. Glendening, C.R. Landis, F. Weinhold, *J. Comput. Chem.* 34 (2013) 1429–1437.
- [30] G. Varadharaj, C.D. Reeve, *Tetrahedron Asymmetry* 9 (1998) 1191–1195.